TECHNICAL MEMORANDUM

214

# The anomalous rainfall over the USA during July 1993 sensitivity to land surface parameterization and soil moisture anomalies

A.C.M. Beljaars, P. Viterbo,
M.J. Miller and A.K. Betts

Research Department

March 1995



European Centre for Medium-Range Weather Forecasts
Europäisches Zentrum für mittelfristige Wettervorhersage
Centre européen pour les prévisions météorologiques à moyen

Abstract

This paper discusses the sensitivity of short and medium-range precipitation forecasts for the central USA to land surface parametrization and soil moisture anomalies. Two forecast systems with different land surface and boundary layer schemes were running in parallel during the extreme rainfall events of July 1993. One forecast system produces much better precipitation forecasts due to a more realistic thermodynamic structure resulting from improved evaporation in an area that is about one day upstream of the area of heaviest rain. The paper also discusses two ensembles of 30 day integrations for July 1993. In the first ensemble soil moisture is initialized at field capacity (100% availability); in the second ensemble at 25% of soil moisture availability. It is shown that the wet integrations produce a much more realistic precipitation pattern than the dry integrations. These results suggest that there may be some predictive skill in the monthly range related to the time scale of the soil moisture reservoir.

## 1. INTRODUCTION

July 1993 showed anomalously high precipitation over the central USA with exceptional flooding of the Mississippi (*Kunkel et al*, 1994). During this month, a new model version (cycle 48, hereafter called CY48) of the ECMWF model with the land surface scheme described by *Viterbo and Beljaars* (1995), ran in parallel with the operational forecast system (model cycle 47; hereafter called CY47). Such parallel runs are used for final testing of system changes prior to operational implementation. The parallel run includes data assimilation and 10 day forecasts with the new model version at operational resolution (T213L31). Comparison of the CY47 and CY48 precipitation forecasts with observations showed that CY48 performed much better. This paper presents some results of this comparison and addresses the reason for the improvement and the relevant role of land surface processes.

Although the two model versions have a number of differences (listed in the next sections), it is believed that the revised land surface scheme is the main contributor to the improved precipitation forecasts. The new scheme does not specify a climatological deep boundary condition for soil moisture and therefore has a much better potential for handling soil moisture anomalies. To illustrate this aspect, sensitivity experiments are also carried out with the new CY48 at T106L31 resolution. An ensemble of three 30 day integrations is initialized with soil moisture at field capacity and compared with a similar ensemble initialized at 25% of soil moisture availability. The "wet" integrations produce much more precipitation than the "dry" integrations, showing that evaporation influences precipitation considerably. These results suggest that there is persistence in the behaviour of precipitation and so there may be seasonal predictability potential related to the depletion time scale of the soil moisture reservoir (*Rowntree and Bolton*, 1983; *Mintz*, 1984).

The treatment of land surface processes in large scale atmospheric models has always been a difficult problem, because of the complicated interactions between atmosphere, vegetation and soil, and the lack of data for different climatological regimes. Current physically based land surface schemes may model atmosphere surface interaction with Monin Obukhov similarity, treat bare soil evaporation as controlled by soil moisture in a shallow top soil layer, treat evaporation from vegetation with a stomatal resistance controlled by soil moisture in the root zone, they may represent potential evaporation from snow and/or an interception reservoir, and they may also represent some sort of soil hydrology (e.g. *Dickinson et al*, 1986; *Sellers et al*, 1986; *Noilhan and Planton*, 1989; *Abramopoulos et al*, 1988; *Blondin*, 1991; *Viterbo and Beljaars*, 1995). These models can vary widely in their implementation depending on the details of the model and the level of complication that is adopted (e.g. vertical resolution in the soil, number of geographically dependent terrain parameters etc.). Although most schemes have been validated and

calibrated with the help of field data, the differences between individual models can still be large, as is becoming increasingly clear from the Project for Intercomparison of Land-surface Parametrization Schemes (PILPS; *Henderson-Sellers et al*, 1993). The behaviour of land surface schemes on the seasonal time scales is less well documented and less well tested than their behaviour on the diurnal time scale.

The impact of land surface processes in General Circulation Models (GCM's) has been studied by *Rowntree and Bolton* (1983), *Dickinson and Henderson-Sellers* (1988), *Nobre et al* (1991), *Lean and Rowntree* (1993), *Atlas et al* (1993) and *Milly and Dunne* (1994) (and reviewed recently by *Garratt*, 1993). *Mintz* (1984) concluded that a coupling exists between evaporation and precipitation in the sense that precipitation increases over land when evaporation increases. This implies a positive feedback from the recirculation of precipitation through the soil moisture reservoir, which may lead to prolonged persistence of anomalous wet or dry spells. Such a persistence was indeed found by *Oglesby* (1991) from model simulations, and suggested in a data study by *Namias* (1958), in which significant lagged correlations were found in the 700 hPa field over the Midwest of the USA between spring and summer, and from a correlation of spring precipitation anomalies and summer temperature anomalies.

Although the precipitation response to evaporation is marked, it is not very clear how this response works in detail. *Rowntree and Bolton* (1983) present the general notion that evaporation increases the moisture content of the troposphere and brings the air closer to saturation and therefore facilitates precipitation. However, given a certain incoming net radiation, soil moisture mainly affects the partitioning of sensible and latent heat flux at the surface. Consequently the equivalent potential temperature ($\theta_e$, determining the condition for convective precipitation) in the boundary layer is not affected by the Bowen ratio at the surface. *Betts et al* (1994) and *Betts and Ball* (1995) demonstrate with observational data and a simple boundary layer model that reduced evaporation, and therefore increased heating at the surface, increases entrainment at the top of the boundary layer and thus increases entrainment of low $\theta_e$ air from above the boundary layer. This leads to lower $\theta_e$ in the boundary layer, a more stable troposphere and might therefore lead to less convective precipitation.

Summer precipitation over the Mississippi basin is closely linked to a persistent flow pattern, sometimes referred to as the USA summer monsoon. Moisture is transported from the Gulf of Mexico in a northward boundary layer flow over Mexico, Texas, and Oklahoma, curving gradually eastward over the plains (*Rasmusson*, 1967, 1968, 1971). Severe storms triggered by upper air disturbances coming from the West, create much of the summer precipitation.

*Benjamin and Carlson* (1986) and *Lanicci et al* (1987) discuss the role of differential advection, with a warm/dry southwesterly flow from the Mexican plateau overlying a moist southerly flow from the Gulf of Mexico, giving a capping inversion which allows the build up of large conditional instability. As a consequence, when the soil is more moist over the Mexican Plateau the heating is smaller, the stabilizing inversion is weaker, and convective precipitation is not inhibited.

In this paper, the short and medium range forecasts with two different land surface schemes are analyzed in order to understand the interaction between evaporation and precipitation. The new scheme produces much better precipitation forecasts due to a more realistic thermodynamic structure in the lower troposphere, which in turn results from improved evaporation in an area that is about one day upstream. Analysis of a small ensemble of 30 day integrations using the new land-surface scheme with different initial conditions

for soil moisture suggests that some predictability exists in the extended range, due to the memory of the soil moisture reservoir.

## 2. MODEL DESCRIPTION

Since 1991, the operational ECMWF model has been a global spectral model using triangular truncation at wave number 213 and an envelope orography. The corresponding Gaussian grid has a maximum of 640 points along a latitude line. The grid point spacing of about 60 km at the equator is roughly maintained towards the poles by reducing the number of points along each latitude (*Hortal and Simmons*, 1991; *Ritchie et al*, 1995). The model has 31 levels in the vertical defined by hybrid coordinates (*Simmons and Strufing*, 1981) with between three to eight levels in the boundary layer at approximately 33, 150, 360, 640, 970, 1360, 1800 and 2290 m above the surface. The physics package consists of the radiation scheme by *Morcrette* (1990), the mass flux convection scheme by *Tiedtke* (1989) and the gravity wave drag scheme by *Miller et al* (1989). The boundary layer scheme and the land surface scheme of Cycle 47 (CY47) are described by *Louis* (1979), *Louis et al* (1982) and *Blondin* (1991) respectively; CY47 provides the control experiment for this study.

The new land surface scheme and the boundary layer scheme used in this paper represent a considerable modification from CY47. The land surface scheme and the surface layer part of the boundary layer scheme are described by *Viterbo and Beljaars* (1995). The main changes with respect to CY47 are summarized in Table 1.

| CY47 | CY48 |
|---|---|
| Two prognostic soil layers (of 7 and 42 cm depth) plus climatological layer (of 42 cm depth) specified as a boundary condition | Four prognostic layers (of 7, 21, 72, and 189 cm depth); zero-heat diffusion and free drainage at the bottom |
| Constant hydraulic conductivity and diffusivity | Hydraulic conductivity and diffusivity dependent on soil moisture allowing rapid infiltration |
| Uses the temperature of the top soil layer for coupling with the turbulent boundary layer and with the radiation scheme | Introduces a skin layer for temperature |
| Same roughness length for heat, moisture and momentum | Roughness length for heat and moisture smaller than for momentum |
| Stability dependent exchange coefficients. No planetary boundary layer (PBL) top entrainment | Diffusion coefficients in the unstable boundary layer prescribed as a similarity profile (*Troen and Mahrt*, 1986; *Holtslag and Boville*, 1993), with no countergradient term. Represents PBL top entrainment as 20% of the surface buoyancy flux (*Beljaars and Betts*, 1993) |

Table 1: Main differences between CY47 and CY48. The details of the land surface schemes are described by *Blondin* (1991) for CY47 and by *Viterbo and Beljaars* (1995) for CY48

Some other changes have been made in CY48 that are of little relevance to the current paper. These include a modification of the lateral entrainment of updrafts in the shallow convection scheme and a decrease of the air-sea transfer coefficients for heat and moisture at high wind speeds.

## 3. THE PARALLEL RUN OF MODEL CYCLES 47 AND 48 IN JULY 1993

In order to carry out a comparison of the two model cycles, the problem of what global soil moisture distribution to commence the experiment had to be addressed. The initialization of soil moisture (for which no global coverage is routinely available) in global forecast models is still a subject of active research (*Bouttier et al*, 1993; *Viterbo and Beljaars*, 1995), however it was realized in preliminary experiments that it is better to commence with relatively wet soil conditions, rather than dry conditions which encourage positive feedbacks as discussed later.

It was therefore decided to initialise the main experiment of CY48 data assimilation system starting from July 2 with the soil moisture at field capacity over vegetated areas. This decision was influenced by the fact that it had been wet over much of the USA and Europe in June. A weighting was applied based on the vegetation cover between field capacity for the vegetated fraction and the multiyear model climate for the bare soil part, so that CY48 assimilation system was started from soil moisture that was at field capacity in vegetated areas. The multiyear model climate was generated by averaging soil moisture month by month from a 5 year integration at T63L31 resolution (see *Viterbo and Beljaars*, 1995).

The CY47 and CY48 data assimilation/forecast systems ran in parallel from 2 July until 22 July 1993, and CY48 became the operational model at the beginning of August. In the following we use averages of analysis and short range forecasts from 9 July to 25 July. The system consists of data assimilation with 6-hour forecasts as first guess for the analysis every 6 hours, and 10 day forecasts every day from the 12 UTC analysis. The results of the first week of the parallel assimilation have been discarded to reduce possible spin-up effects from the soil moisture initial condition.

### 3.1 **Precipitation**

The precipitation and anomaly maps for July 1993 as published in the Weekly Weather and Crop Bulletin are shown in Fig 1. There is a large area over the centre of the USA covering Kansas, Nebraska, Missouri, and Iowa, where the precipitation is twice the normal amount. The states along the Canadian border west of the Great Lakes also have anomalously high precipitation. However, parts of the south (e.g. a large portion of Texas) and the east of the USA are anomalously dry.

In the following plots we will show precipitation (and evaporation) amounts from 0 to 24, 24 to 48 and 48 to 72 hour forecasts from consecutive days averaged from 9 to 25 July according to verifying date. Comparison of the CY47 and CY48 data assimilation/forecast system showed that the precipitation of day 1 of the forecasts were accurate and very similar. Differences developed between the forecasts from day 2 onwards. This suggests that precipitation in the very short range (and also in the first guess during data assimilation) is not very sensitive to the land surface scheme but is mainly determined by the analysed initial fields which are constrained by observations. However, the precipitation for day 3 of the forecasts already has pronounced differences. We compared the averages over all 48 to 72 hour forecasts verifying from 9 to 25 July with SYNOP observations (Fig 2). The observations are shown as printed numbers. The data of Fig 2 covers only 17 days of July, but still shows a precipitation anomaly similar to the monthly patterns

of Fig 1. Fig 2 shows that the CY48 model captures the precipitation maximum in the centre of the USA much better than CY47. The differences in precipitation and evaporation between CY48 end CY47 are shown in Fig 3 for the 48-72 hour time range. The differences in evaporation are substantial, but not at the same locations as the differences in precipitation. For instance the western part of the USA and Mexico have up to 4 mm/day more evaporation with CY48. However, the difference in evaporation is rather small in the area with the maximum difference in precipitation. The fact that the differences in precipitation and evaporation are not highly correlated is important for it implies that the differences in precipitation are not tied to local differences in evaporation and vice-versa.

To examine the differences in spin-up between CY47 and CY48 we compute averages of precipitation and evaporation over the area between 35-45 N and 90-100 W for different time ranges (see Table 2). CY47 has more than 6 mm/day of precipitation in this area during the first 24 hours of the forecast and the precipitation gradually spins down to about 2 mm/day at day 5. The new model (CY48) also has more than 6 mm/day during the first 24 hours but it maintains the rate of precipitation much better during the forecast up to day five. Evaporation in this area is very similar with both models and virtually independent of forecast range. It suggests that local recirculation as proposed by *Betts et al* (1994) cannot explain the difference between the two models since a local recirculation mechanism would imply a spindown of evaporation in CY47.

| | forecast range (hours) | Precipitation (P) (mm/day) | Evaporation (E) (mm/day) | P-E (mm/day) |
|---|---|---|---|---|
| CY48 | 0-24 | 6.62 | 4.45 | 2.17 |
| | 24-48 | 7.71 | 4.67 | 2.44 |
| | 48-72 | 5.56 | 4.50 | 1.06 |
| | 96-120 | 5.08 | 4.62 | 0.46 |
| CY47 | 0-24 | 6.42 | 4.41 | 2.01 |
| | 24-48 | 4.79 | 4.60 | 0.19 |
| | 48-72 | 2.60 | 4.60 | -2.00 |
| | 96-120 | 1.92 | 4.36 | -2.44 |

Table 2: Precipitation and evaporation from the July parallel run at different forecast ranges with CY47 and CY48 at T213L31 resolution averaged over the area between 35-45 N and 90-100 W and over all forecasts verifying between 9 and 25 July 1993.

### 3.2 **Thermodynamic profiles**

To gain insight into the mechanism responsible for the precipitation difference in the two model versions, we plot the mean of the forecast thermodynamic profiles at different forecast ranges near 40 N, 95 W (which is close to the NE corner of Kansas, where the July precipitation was heaviest) (Fig 4). These profiles are taken from model levels starting at about 30 m above the surface. We selected the 6, 30 and 78 hour forecasts because these correspond to approximate local noon. The short-range forecasts (verifying at 18 UTC) of CY48 and CY47 (Fig 4a,b) are very similar (apart from some details of the boundary layer structure), which indicates that they are still close enough to the analysis time that differences have yet to develop. The two sets of analyses are quite similar, since in this data rich area the analysis relies little on the background field (6 hour forecasts) and the data always defines a realistic analysis structure. However

at the forecast range of 30 hours, (Fig 4c,d) very distinct differences can now be seen between the two model versions. These differences continue to develop later in the forecast (Fig 4e,f). The reason that CY47 produces less precipitation than CY48 is that a pronounced inversion develops at about 900 hPa in the CY47 forecasts. The air at 850 hPa is too dry and too warm in CY47, which is clear from a comparison of the profiles with the 6 hour forecasts (we interpret the 6 hour forecast as an analysis here; the model analysis of 18 UTC is hardly different because no radiosondes are launched at this synoptic hour). The profiles at different forecast ranges are much more similar in the CY48 forecasts than they are in the CY47 forecasts, with the model formulation of CY48 maintaining the observed thermodynamic structure much better than CY47.

To trace the development of these differences in structure, three day backward trajectories have been computed from 40N, 95 W at different vertical levels. The time averaged CY48 forecast fields at the successive time ranges of 72, 66, 60, 54, ..., 12, 6, and 0 hours, have been used to go three days back in time (see Fig 5). The same has been carried out with the fields from CY47 with very similar results to Fig 5, and are therefore not reproduced here. The boundary layer air at 40 N 95 W originates over the Gulf of Mexico two days earlier and follows a slightly subsiding motion. This is the well known source for moisture supply over the Central USA referenced earlier. There is however considerable wind shear, with the 850 hPa air following a more westward trajectory than the near surface air and therefore experiencing the influence of the land surface over a much longer distance. This differential advection plays an important role in the formation of the inversion in the area with maximum precipitation.

The time evolution of the 850 hPa temperature difference between the two sets of forecasts is shown in Fig 6. There is little difference between the two systems after 6 hours. Within 12 hours (0 UTC, about 1800 hours local time), a pronounced difference has already developed, with maximum values around 2 K. The area with largest temperature differences coincides with the area of largest evaporation differences shown in Fig 3b, and is the result of differences in daytime heating from the surface. During the night the extent of the maximum temperature difference decreases and moves gradually northeastwards from about 33 N 99 W, along the trajectories shown in Fig 5. The next day (forecast range 30 hours at local noon), the area of largest temperature difference at 850 hPa is already close to the area with maximum precipitation difference. These results strongly suggest that the precipitation difference at day 2 and 3 between the two model cycles is caused by differences in surface heating one day earlier in an area upstream.

It is not easy to say which forecast system has the correct surface heating, since direct observations of surface fluxes are not available. Air parcels at 850 hPa in a 10x10 box centred at 40 N 95 W have moved about 700 km in 24 hours (see Fig 5). As indirect evidence for the quality of surface fluxes we compare in Fig 7 the model two-metre temperature, $T_2$, and specific humidity, $q_2$, with SYNOP observations in the area 35-45 N and 90-100 W, where the precipitation difference between CY47 and CY48 is larger. For each day between July 9-25 observed values are displayed, together with the corresponding 54, 60, 66, and 72-hour forecast. Fig 8 shows a similar plot for the area 28-38 N and 93-103 W, displaced 24 hours upstream. The two areas have a small overlap, with 18 SYNOP stations in Fig 7, 17 SYNOP stations in Fig 8, and 3 stations in common.

Figs 7 and 8 show a number of major differences, and it is clear that CY48 reproduces the observed specific humidity much better than CY47 in both areas, as CY48 is moister and has a smaller diurnal cycle. This improvement is due to the combined effect of more moisture supply from the surface and the entrainment

of dry air at the top of the boundary layer in CY48, which gives a more realistic diurnal cycle. The daytime temperatures are lower with CY48 than with CY47, which is also an improvement. The daytime temperatures are particularly important for medium range forecasting since daytime temperature errors can penetrate over deep layers and therefore affect the synoptic pressure fields. Finally there is a small increase in the amplitude of the diurnal cycle for temperature in CY48, which makes the night time temperatures too low. The night time cooling is connected to the parametrization of the stable boundary layer, which is currently under investigation (see *Beljaars*, 1995 for more diagnostics). Excessive night time cooling is less critical for medium range forecasting since only very shallow near-surface layers are affected.

From the comparison with SYNOP temperature and specific humidity we conclude that the new CY48 has a clear beneficial impact on atmospheric heat and moisture budgets, and it is therefore likely that the surface fluxes of heat and moisture are better represented with CY48 than with CY47.

In summary, it is concluded that the large precipitation differences are the result of differences in surface heating in the area one day upstream, impacting on the atmospheric thermodynamic structure. Increased evaporation and reduced heating in moist soil conditions upstream result in the absence of significant boundary layer capping inversion and hence little inhibition of deep precipitating convection.

## 4. EXTENDED INTEGRATIONS WITH DIFFERENT INITIAL CONDITIONS FOR SOIL MOISTURE

In the previous section we have seen that precipitation is little correlated with local evaporation, but strongly influenced by evaporation upstream. But evaporation is controlled by soil moisture availability, and precipitation refills the soil moisture reservoir, so we clearly have a positive feedback loop. The time scale for soil moisture depletion is not simply determined by the size of the soil moisture reservoir divided by the evaporation rate (e.g. 150 mm divided by 3 to 5 mm/day), but by the soil moisture reservoir divided by evaporation minus precipitation. With a tight coupling between evaporation and precipitation such a time scale can become very long, leading to persistent dry or wet conditions. In climate models and models for seasonal forecasting, the realism of the coupling is obviously crucial in obtaining a realistic seasonal evolution of soil moisture, precipitation and evaporation. In data assimilation/forecast systems such as the ECMWF (CY48) system it is also relevant since the soil moisture is controlled by precipitation and evaporation from short range (6 hrs) forecasts during assimilation, with no soil moisture data.

Since the soil was nearly saturated on 1 July over large areas of the USA, it is interesting to consider the sensitivity of longer integrations to initial soil moisture conditions. This will also give some insight into the interaction of precipitation with soil moisture and in the time scale of soil moisture depletion. For this purpose we use two ensembles of three 30-day integrations with CY48 at T106L31 resolution. The ensembles consisted of 30 day forecasts starting from 1, 2 and 3 July using the analyses from the parallel run with CY48. The two ensembles differ only in their initial soil moisture conditions. The forecasts from the first ensemble were initialized at field capacity, whereas the second ensemble was initialized at 25% availability ($\theta=\theta_{pwp}+0.25(\theta_{cap}-\theta_{cap})$, where $\theta_{cap}$ is the field capacity and $\theta_{pwp}$ is the permanent wilting point of the soil; see *Viterbo and Beljaars*, 1995 for the vegetation model). The precipitation and evaporation maps averaged over 30 days and over the three members of the ensemble are shown in the Figs 9 and 10. The water budgets over the area 35-45 N and 90-100 W are given in Table 3. The precipitation difference over the central USA is pronounced (Fig 9), although the area with maximum difference is slightly more to the north than in the operational parallel run (compared with Fig 3a) and also in comparison with the

observed anomaly of July 1993 (compare with Fig 1a). The evaporation is considerably higher over large areas with the wet initial condition, particularly in the south-central USA (Fig 10). Table 3 shows the precipitation and evaporation balance for the area between 35-45 N and 90-100 W. The difference is striking. With a wet initial soil moisture, both evaporation and precipitation are roughly double the values with the dry initial soil moisture. In the long term averages, P and E are more closely in balance, so the relative role of nonlocal effects is less obvious. On the USA-Canadian border west of the Great Lakes, there is only a marginal increase of evaporation with the moist soil moisture initialization, whereas the precipitation shows an increase of more than 2 mm/day in the same area. In the south-central US, E increases over a large area, where P increases are smaller. Thus it appears that the precipitation increase in the central USA is linked to the evaporation difference upstream as in the short term forecasts discussed in section 3.

| | Initial date | Precipitation (P) (mm/day) | Evaporation (E) (mm/day) | P-E (mm/day) |
|---|---|---|---|---|
| Wet | 930701 | 4.07 | 4.54 | -0.47 |
| | 930702 | 3.70 | 4.39 | -0.69 |
| | 930703 | 4.00 | 4.48 | -0.48 |
| | Ensemble mean | 3.92 | 4.47 | -0.55 |
| Dry | 930701 | 1.69 | 2.19 | -0.50 |
| | 930702 | 2.14 | 2.26 | -0.12 |
| | 930703 | 2.16 | 2.22 | -0.06 |
| | Ensemble mean | 2.00 | 2.22 | -0.22 |

Table 3: Precipitation and evaporation from the ensemble of wet and dry long runs with CY48 at T106L31 resolution averaged over 720 hours and the area between 35-45 N and 90-100 W.

The 18 UTC (about local noon) thermodynamic profiles for the location 40 N, 95 W are shown in Fig 11 for the wet and dry ensemble for comparison with the operational analysis (CY47). We compare with the analysis because no radiosondes are available at 18 UTC. A disadvantage is that the analysis is mainly determined by the background field produced by the 6 hour forecast of the data-assimilation system. We can not have confidence in detailed boundary layer structures of the analysis as it is mainly determined by the parametrizations of the model. We know for instance that the boundary layers in the operational model tend to be too shallow (cf. *Betts et al*, 1993). However, temperature and moisture over deep layers are more reliable since they are heavily constrained by data (every 12 hours) in the assimilation system as is also clear from a comparison of two different systems in the Figs 4a and 4b. The profiles in Fig 11 are averages over 30 days of the forecasts and the 3 members of the ensemble for 18 UTC. It is clear that the integration from the wet initial soil moisture has a much more realistic thermodynamic structure. In contrast, the integrations from the dry initial condition produce a very deep and dry mixed layer structure, with little or no conditional instability. Although the wet integration is rather realistic in its moisture profile and in its general profile structure, the temperature is too low by a few degrees over the layer from 900 to 600 hPa. The dry integration is too dry and too warm from the surface up to 700 hPa. That even the wet integrations have deeper mixed layers than the operational analysis is probably related to the difference in boundary layer entrainment in CY48 and CY47 of the assimilation system.

To allow a direct comparison with radiosondes we also reproduce the 0 UTC profiles (late afternoon local time) averaged over the ensemble and the month of July (Fig 12, 13). Two stations have been selected near 40 N 95 W together with the model output at the gridpoint nearest to the station. A similar picture emerges. The wet integration is more realistic in its moisture profile and general structure and the temperature is too low. The dry integration has an unrealistic deep mixed layer with a boundary layer that is too dry and too warm. This general picture applies to both stations, but the stations show differences as well. Station 72553 (Fig 12C) which is only about 250 km north of station 72456 (Fig 13C) is systematically cooler by a few degrees. This north-south temperature gradient is at least partially reflected in the wet and dry model integrations.

The marked difference between the wet and dry integrations is also clear from the 850 HPa temperature fields. Fig 14 shows the difference of the two cases from the operational analysis and the difference between wet and dry runs. The dry integration is too warm over the northern part of the USA and Canada. The wet integration is systematically cooler, but compared to the analysis, a little too cold cross the central US.

Trajectories have been computed from wind fields averaged over 30 days and over the three members of the ensemble. The diurnal cycle is retained in the averages by taking the averages separately for 0, 6, 12 and 18 UTC. Fig 15 shows the 3 day backward trajectory from 40 N, 95 W for the wet as well as the dry integrations. Both trajectories show similar flow patterns to the averaged operational trajectory in Fig 5, in spite of being beyond the range of predictability of the synoptic systems, indicating that the monsoon-type flow with low level moisture supply from the Gulf of Mexico was a very robust feature of the local climate for this month.

We conclude that the time scales of soil moisture depletion over the USA implied by these experiments using CY48 of the ECMWF model are very long. This is due to the coupling between precipitation and evaporation which have an average difference over the central USA of around 0.5 mm/day only. It therefore takes a long time for the soil to dry out. However, when the soil is already dry, this dryness persists. The current results suggest that the effect of evaporation on precipitation is somewhat similar to the mechanism we have seen from the short range forecasts, but much more study with larger ensembles and other years/seasons would be needed to give full justice to this complex problem.

## 5. CONCLUSIONS

Results have been presented for July 1993 for the two forecast systems that were running in parallel at ECMWF. The operational system (CY47) has a land surface scheme that is heavily constrained by the deep soil climatological boundary condition for soil moisture and temperature. The new system (CY48) produces its own soil moisture by integrating the soil variables with input from the atmospheric model (e.g. precipitation and evaporation) in the short range. In this way it has the potential to simulate soil moisture anomalies. The new system also has a different formulation for the mixed layer in which a dry entrainment formulation is used. The pre-operational parallel run of CY47 and CY48 showed that the anomalous precipitation over the centre of the USA was captured much more realistically in the 72 hour time range with the new model version. The area with large precipitation differences has only small differences in evaporation, indicating that the local moisture supply is not the controlling factor. Inspection of the thermodynamic profiles indicates unrealistically strong inversions with CY47, capping the boundary layer moisture, and inhibiting the development of convective precipitation. It is deduced that these unrealistic

inversion structures develop as the result of excessive heating upstream of the area of interest. The new model version produces less heating because more moisture is available for evaporation. In this way evaporation affects precipitation in the downstream area, similar to the mechanism proposed by *Benjamin and Carlson* (1986) and *Lanicci et al* (1987). Also *Rowntree and Bolton* (1983) observe downstream propagation of moisture anomalies in their simulations for the European area.

The second part of this paper shows the result of two ensembles of 30 day integrations for July 1993 using the model CY48. The purpose of these experiments is to study the ability of the model to maintain soil moisture. Soil moisture in the first ensemble is initialized at field capacity, whereas the second ensemble is initialized at 25% availability. The wet integrations show much more realistic precipitation for the month of July, but now the evaporation is also quite different. On these longer time scales precipitation and evaporation are more closely in balance locally, and it is more difficult to separate cause and effect. However, the mechanism as diagnosed in the first part of the paper, namely that the difference in precipitation in the central USA is linked to a difference in thermodynamic structure associated with evaporation differences upstream is equally valid in these longer timescales.

Irrespective of the detailed mechanism responsible (which is hard to determine in 30-day ensemble means), these sensitivity experiments indicate a pronounced feedback between land surface hydrology and precipitation on large space and long time scales, associated with the memory of the land surface boundary condition. There is clear indication of predictive skill in the monthly timescale resulting from the long time constant of the soil moisture reservoir. This result underlines the importance of the observation and analysis of soil moisture (e.g. *Bouttier et al*, 1993).

ACKNOWLEDGEMENTS

The authors would like to thank Dr Andreas Lanzinger for providing the operational data for some of the diagnostics in this paper. Alan Betts has been supported by NSF under ATM90-01960 and NASA-GSFC under contract NAS5-31738, and NAS5-32356. Our colleagues at ECMWF, Drs Tony Hollingsworth and Adrian Simmons, read the manuscript and gave valuable suggestions for improvements.

REFERENCES

Abramopoulos, F, C Rosenzweig and B Choudhury, 1988: Improved ground hydrology calculations for global models (GCM's): soil water movement and evapotranspiration. J Climate, **1**, 921-941.

Atlas, R, N Wolfson and J Terry, 1993: The effect of SST and soil moisture anomalies on GLA model simulations of the 1988 US summer drought. J Climate, **6**, 2034-2048.

Beljaars, A C M and A K Betts, 1993: Validation of the boundary layer scheme in the ECMWF model. Proc Seminar ECMWF, 7-11 September 1992, Reading, UK, ECMWF, Vol II, 159-195.

Beljaars, A C M, 1995: The impact of some aspects of the boundary layer scheme in the ECMWF model. Proc Seminar ECMWF, 5-9 September 1994, Reading, UK, ECMWF.

Benjamin, S G and T N Carlson, 1986: Some effects of surface heating and topography on the regional severe storm environment. Part I: Three-dimensional simulations. Mon Wea Rev, **114**, 307-329.

Betts, A K, J H Ball and A C M Beljaars, 1993: Comparison between the land surface response of the European Centre model and the FIFE-1987 data. Quart J Roy Meteor Soc, **119**, 975-1001.

Betts, A K and J H Ball, 1995: The FIFE surface diurnal cycle climate. J Geophys Res, in press.

Betts, A K, J H Ball, A C M Beljaars, M J Miller and P Viterbo, 1994: Coupling between land-surface boundary-layer parametrizations and rainfall on local and regional scales: Lessons from the wet summer of 1993. Fifth Conference on global change studies, Amer Meteor Soc, 74th Ann Meeting, Nashville, Tenn, 174-181.

Blondin, C 1991: Parametrization of land-surface processes in numerical weather prediction. Land surface evaporation - Measurement and parametrization, T J Schmugge and J-C Andre, Eds, Springer-Verlag, 31-54.

Bouttier, F, J-F Mahfouf and J Noilhan, 1993: Sequential assimilation of soil moisture from atmospheric low-level parameters, Part II: Implementation in a mesoscale model. J Appl Meteor, **32**, 1352-1364.

Dickinson, R E, A Henderson-Sellers, P J Kennedy and M F Wilson, 1986: Biosphere atmosphere transfer scheme (BATS) for the NCAR community climate model. NCAR Tech Note, NCAR/TN-275+STR, 69 pp.

Dickinson, R E and A Henderson-Sellers, 1988: Modelling tropical deforestation: A study of GCM land-surface parametrizations. Quart J Roy Meteor Soc, **114**, 439-462.

Garratt, J R, 1993: Sensitivity of climate simulations to land-surface an atmospheric boundary-layer treatments- A review. J Climate, **6**, 419-449.

Henderson-Sellers, A, Z-L Yang and R E Dickinson, 1993: The project for intercomparison of land-surface parametrization schemes. Bull Amer Meteor Soc, **74**, 1335-1349.

Holtslag, A A M and B A Boville, 1993: Local versus nonlocal boundary-layer diffusion in a global climate model. J Climate, **6**, 1825-1842.

Hortal, M and A J Simmons, 1991: Formulation of the ECMWF model. Mon Wea Rev, **119**, 1057-1074.

Kunkel, K E, S A Changnon and J R Angel, 1994: Climate aspects of the Mississippi river basin flood. Bull Amer Meteor Soc, **75**, 811-822.

Lanicci, J M, T N Carlson and T T Warner, 1987: Sensitivity of the great plains severe-storm environment to soil-moisture distribution. Mon Wea Rev, **115**, 2660-2673.

Lean, J and P R Rowntree, 1993: A GCM simulation of the impact of Amazonian deforestation on climate using an improved canopy representation. Quart J Roy Meteor Soc, **119**, 509-530.

Louis, J-F, 1979: A parametric model of vertical eddy fluxes in the atmosphere. Bound-Layer Meteor, **17**, 187-202.

Louis, J-F, M Tiedtke and J-F Geleyn, 1982: A short history of the operational PBL-parametrization at ECMWF. Proc Workshop ECMWF 25-27 November 1981, Reading, UK, ECMWF, 59-80.

Miller, M J, T N Palmer and R Swinbank, 1989: Parametrization and influence of subgrid-scale orography in general circulation and numerical weather prediction models. Meteor Atmos Phys, **40**, 84-109.

Milly, P C D and K A Dunne, 1994: Sensitivity of the global water cycle to the water-holding capacity of land. J Climate, **7**, 506-526.

Mintz, Y, 1984: The sensitivity of numerically simulated climates to land-surface boundary conditions. The global climate, J Houghton, Ed, CUP, 79-105.

Morcrette, J-J, 1990: Impact of changes in the radiation transfer parametrization plus cloud optical properties in the ECMWF model. Mon Wea Rev, **118**, 847-873.

Namias, J, 1958: Persistence of mid-tropospheric circulations between adjacent months and seasons. The atmosphere and sea in motion (Rossby memorial volume), B Bolin, Ed, Rockfeller Institute Press, 240-248.

Nobre, C A, P J Sellers and J Shukla, 1991: Amazonian deforestation and regional climate change. J Climate, **4**, 957-988.

Noilhan, J and S Planton, 1989: A simple parametrization of land surface processes for meteorological models. Mon Wea Rev, **117**, 536-549.

Oglesby, R J, 1991: Springtime soil moisture variability, and North American drought as simulated by the NCAR Community Climate Model I. J Climate, **4**, 890-897.

Rasmusson, E M, 1967: Atmospheric water vapour transport and the water balance of North America, Part I: Characteristics of water vapour field. Mon Wea Rev, **95**, 403-426.

Rasmusson, E M, 1968: Atmospheric water vapour transport and the water balance of North America: II Large-scale water balance investigations. Mon Wea Rev, **96**, 720-734.

Rasmusson, E M, 1971: A study of the hydrology of Eastern North America using atmospheric vapour flux data. Mon Wea Rev, **99**, 119-135.

Ritchie, H, C Temperton, A J Simmons, M Hortal, T Davies, D Dent and M Hamrud, 1995: Implementation of the Semi-Lagrangian method in a high resolution version of the ECMWF forecast model. Mon Wea Rev, in press.

Rowntree, P R and J A Bolton, 1983: Simulation of the atmospheric response to soil moisture anomalies over Europe. Quart J Roy Meteor Soc, **109**, 501-526.

Sellers, P, Y Mintz, Y C Sud and A Dalcher, 1986: A simple biosphere model (SiB) for use with general circulation models. J Atmos Sci, **43**, 505-531.

Simmons, A J and R Strufing, 1981: An energy and angular-momentum conserving scheme, hybrid coordinates and medium-range weather prediction. ECMWF Tech Rep, No. 28, Reading, UK.

Tiedtke, M, 1989: A comprehensive mass flux scheme for cumulus parametrization in large-scale models. Mon Wea Rev, **117**, 1779-1800.

Troen, I and L Mahrt, 1986: A simple model of the atmospheric boundary layer; sensitivity to surface evaporation. Bound-Layer Meteor, **37**, 129-148.

Viterbo, P and A C M Beljaars, 1995: A new land surface parametrization scheme in the ECMWF model and its validation. Submitted to J Climate.

a)

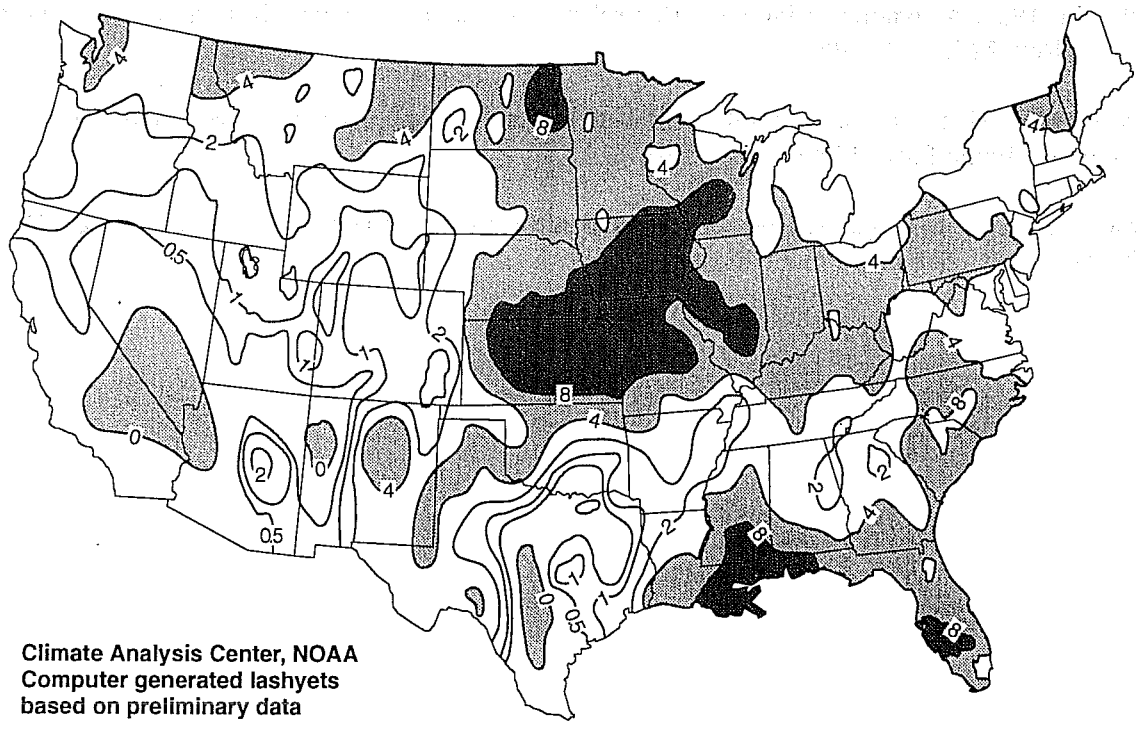


b)

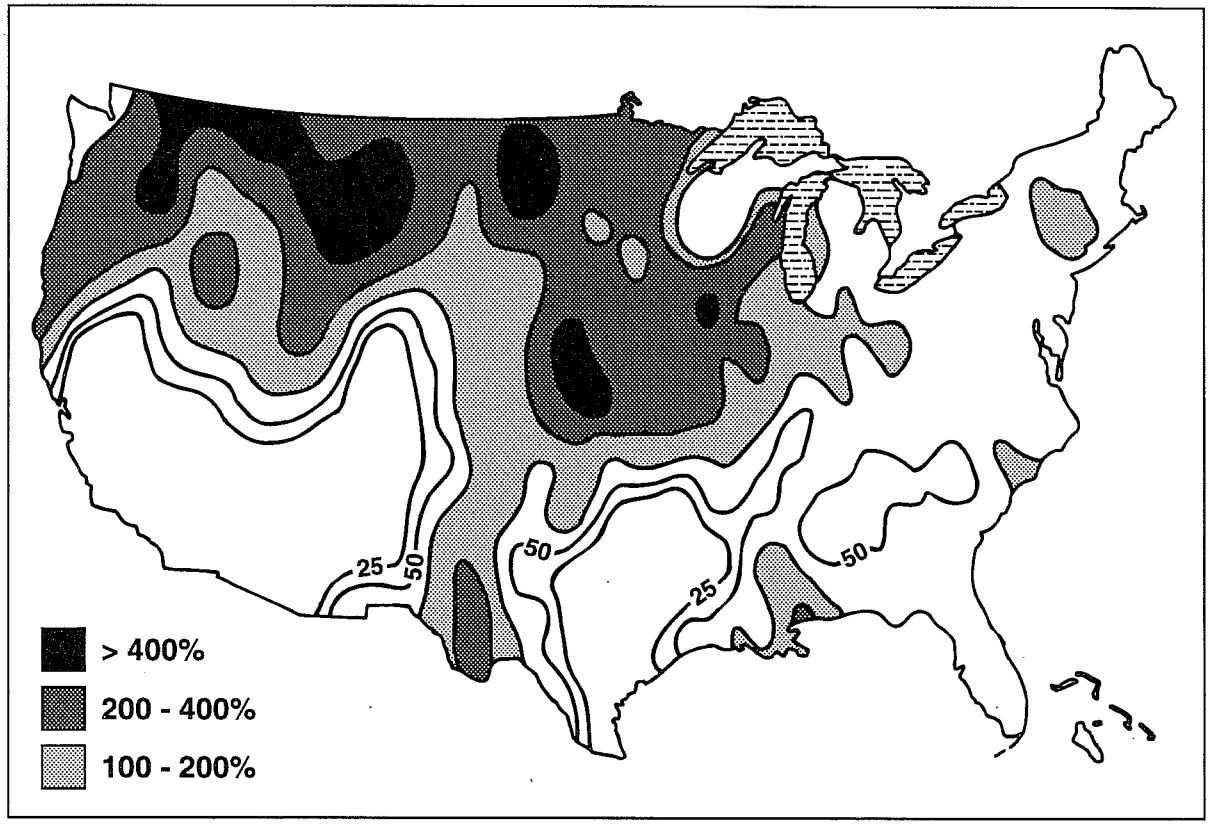


Fig 1 Total precipitation over the USA for July 1993 (A) and the percentage of normal precipitation (B) as published by the Weekly Weather and Crop Bulletin (August 3, 1993). The contours in Fig A are at 0.5, 1, 2, 4, and 8 inches with light and heavy shading above 4 and 8 inches respectively; Fig B has contours at 25, 50, 100, 200, and 400%; with shading above 100%.

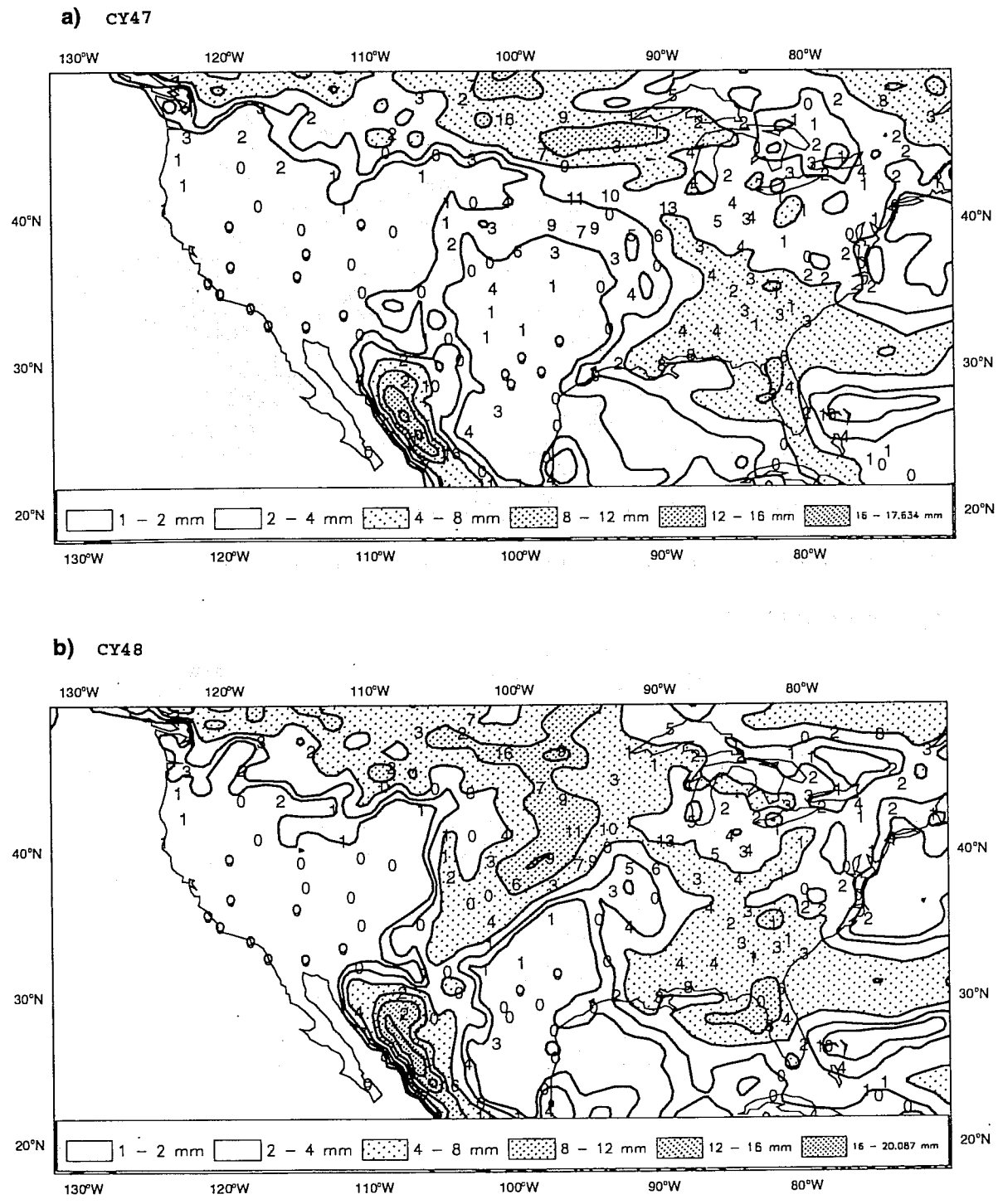


Fig 2 Mean forecast precipitation of all 48 to 72 hour forecasts verifying between 9 and 25 July, with CY47 (A) and with CY48 (B). The contours are at 1, 2, 4, 8 .. mm/day. The printed numbers are station observations in mm/day.

**a)** Precip: CY48-CY47

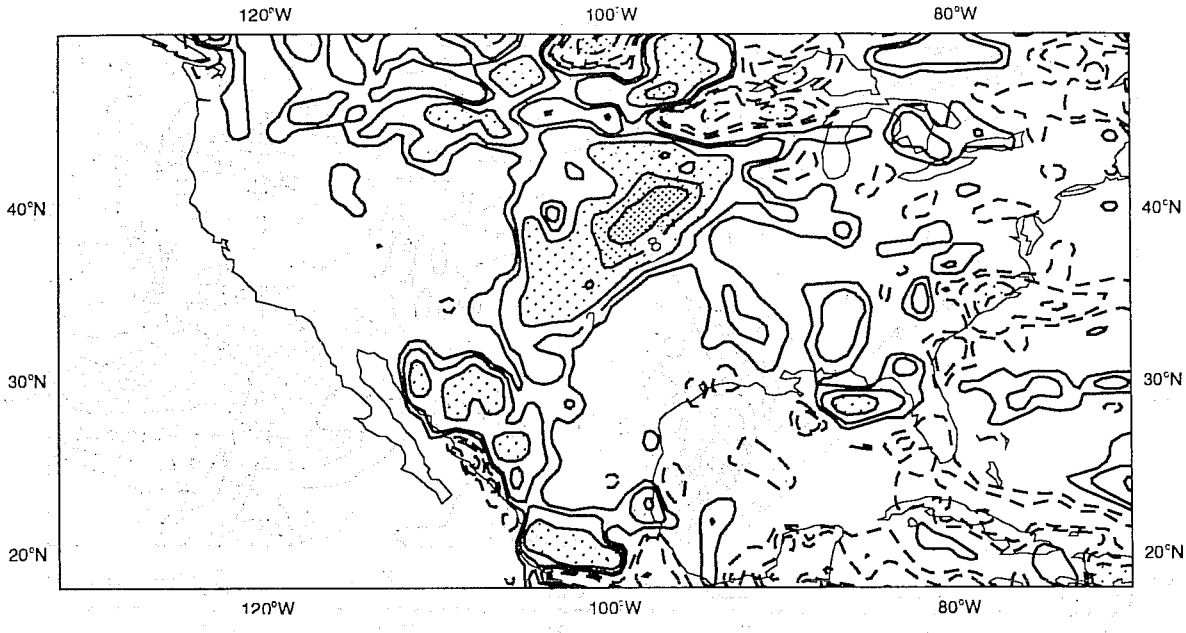


**b)** Evap: CY48-CY47

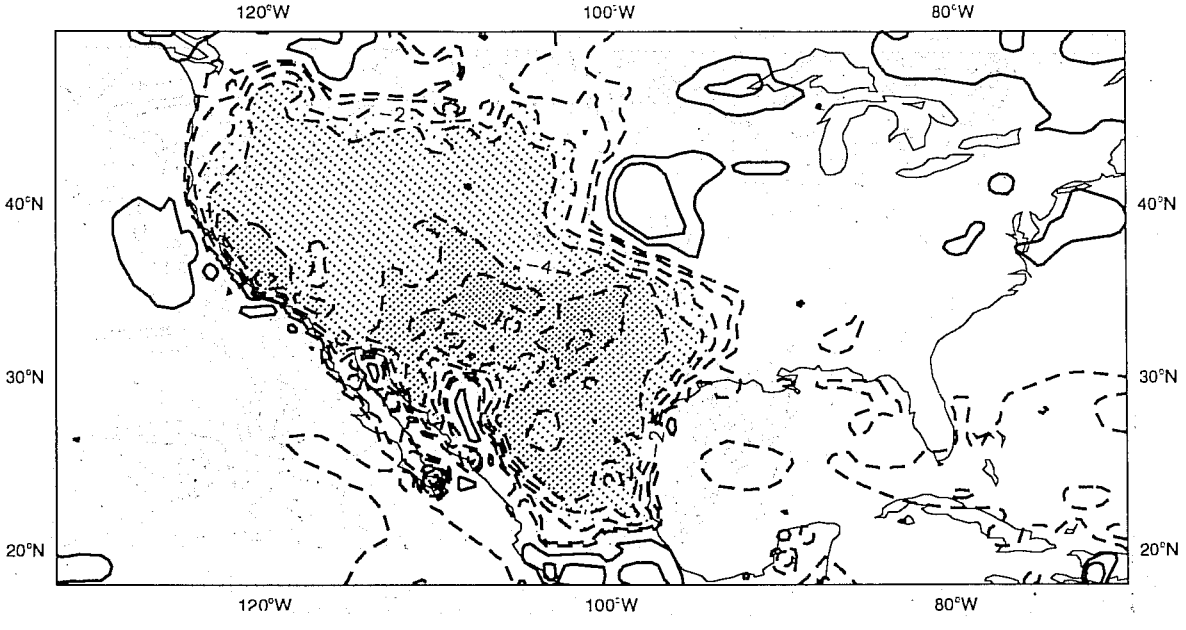


Fig 3 Difference between CY48 and CY47 of the 48 to 72 hour precipitation (A) and evaporation (B), averaged over verifying dates between 9 and 25 July 1993. Dashed contours indicate negative values, which imply an increase for evaporation (by model convention all downward fluxes are positive). The contours for precipitation (A) are at 1, 2, 4, 8, ... with shading above 4 mm/day and for evaporation (B) at 0.5, 1, 2, 3 ...with shading above 2 mm/day.

a) CY47, 6 hour forecasts

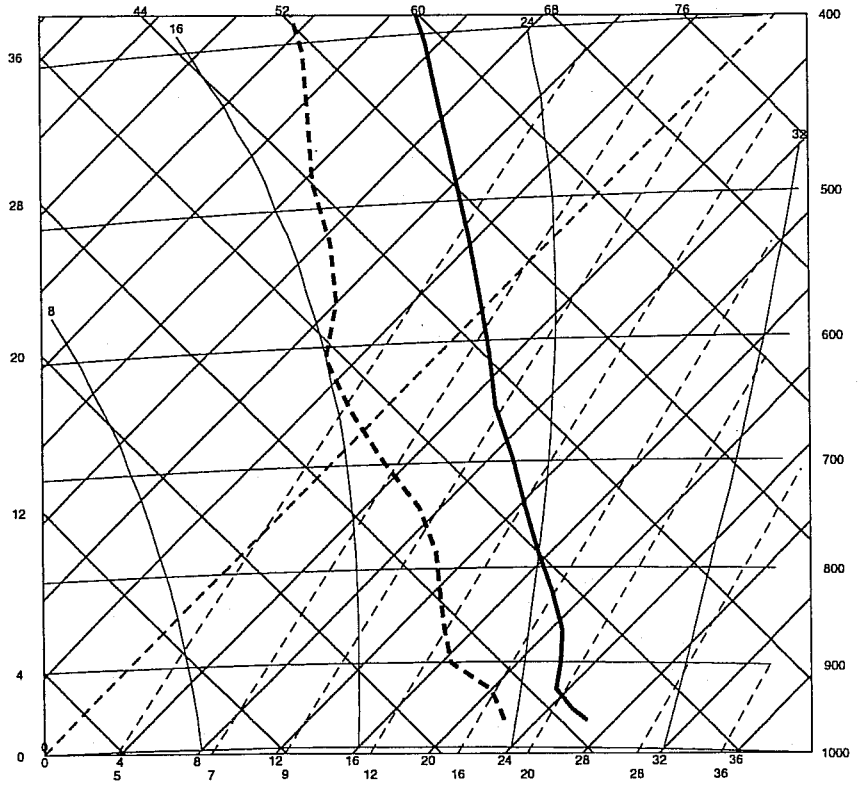


b) CY48, 6 hour forecasts

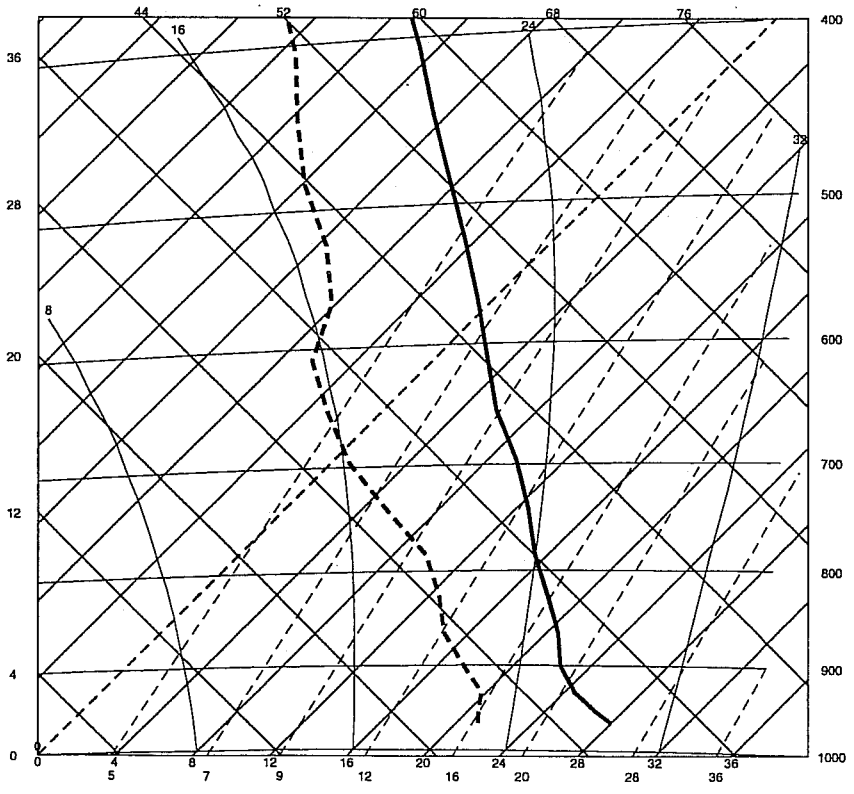


Fig 4 Thermodynamic profiles with CY47 and CY48 of the averages verifying from 9 to 25 July at the forecast ranges of 6, 30 and 78 hours. The location is 40 N, 95 W.

c) CY47, 30 hour forecasts

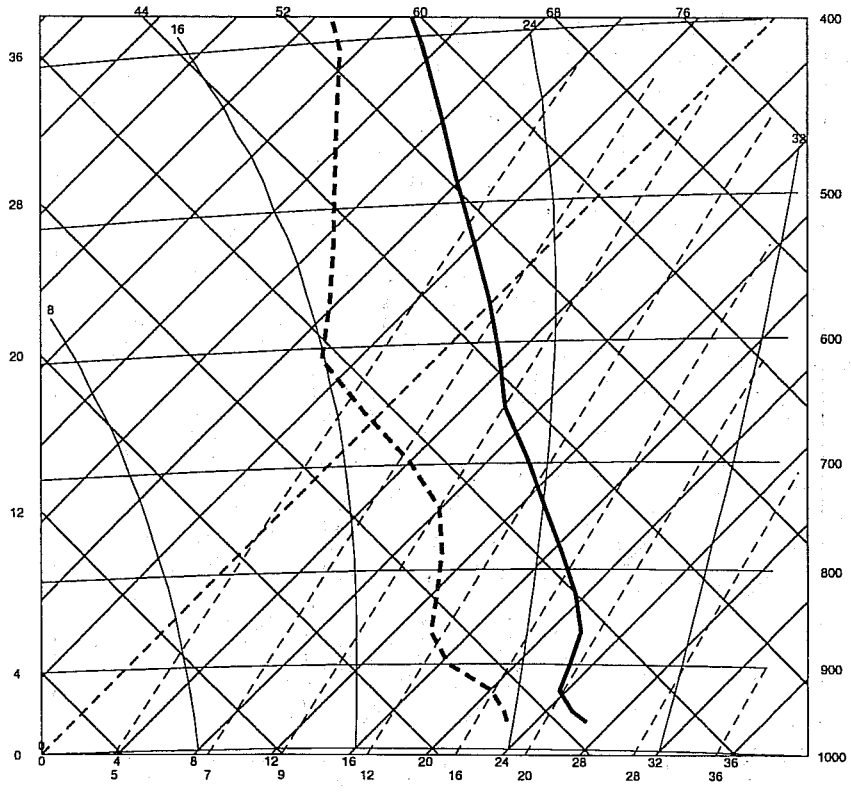


d) CY48, 30 hour forecasts

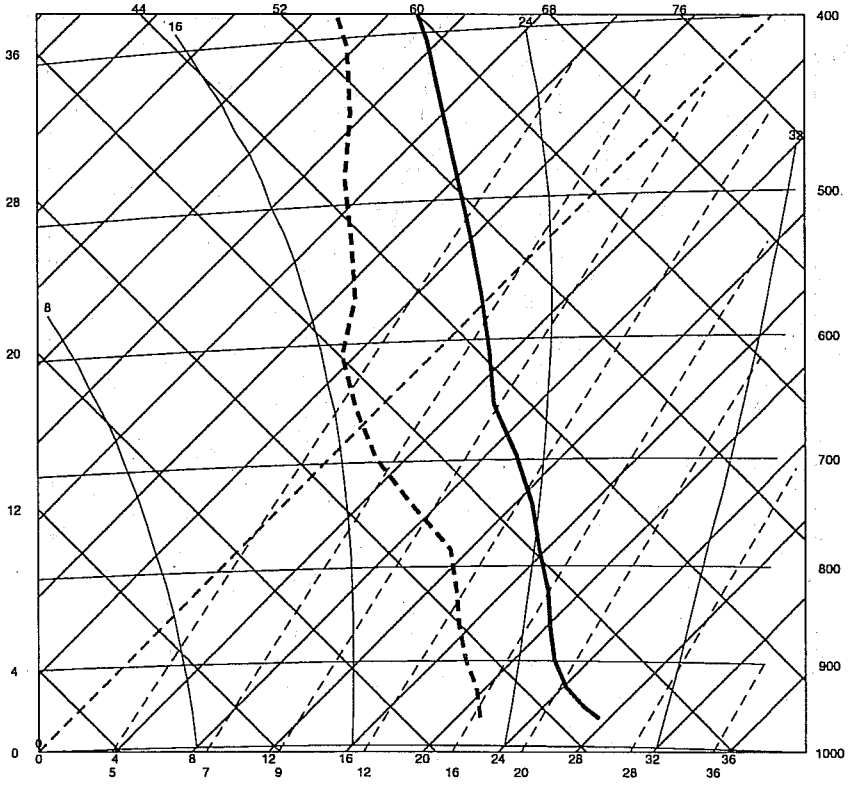


Fig 4 cont.

**e) CY47, 78 hour forecasts**

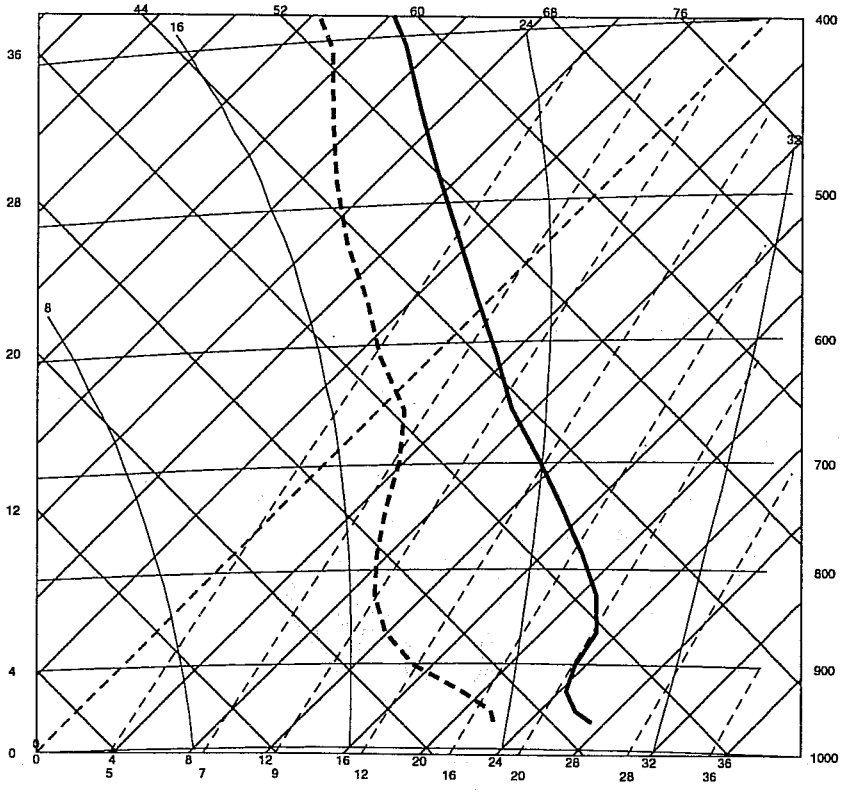


**f) CY48, 78 hour forecasts**

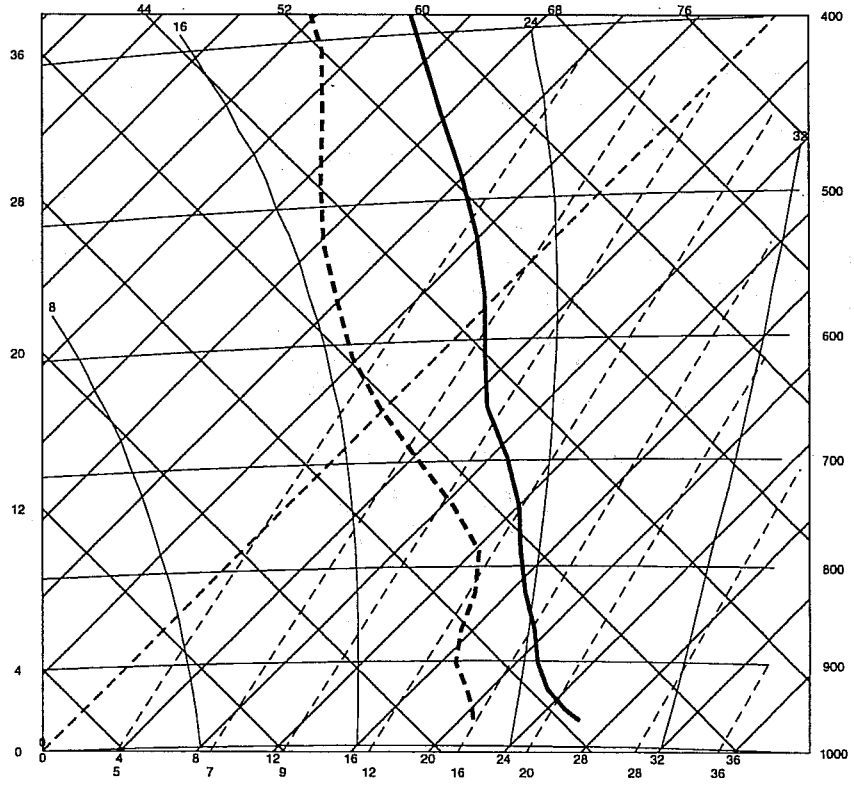


Fig 4 cont.

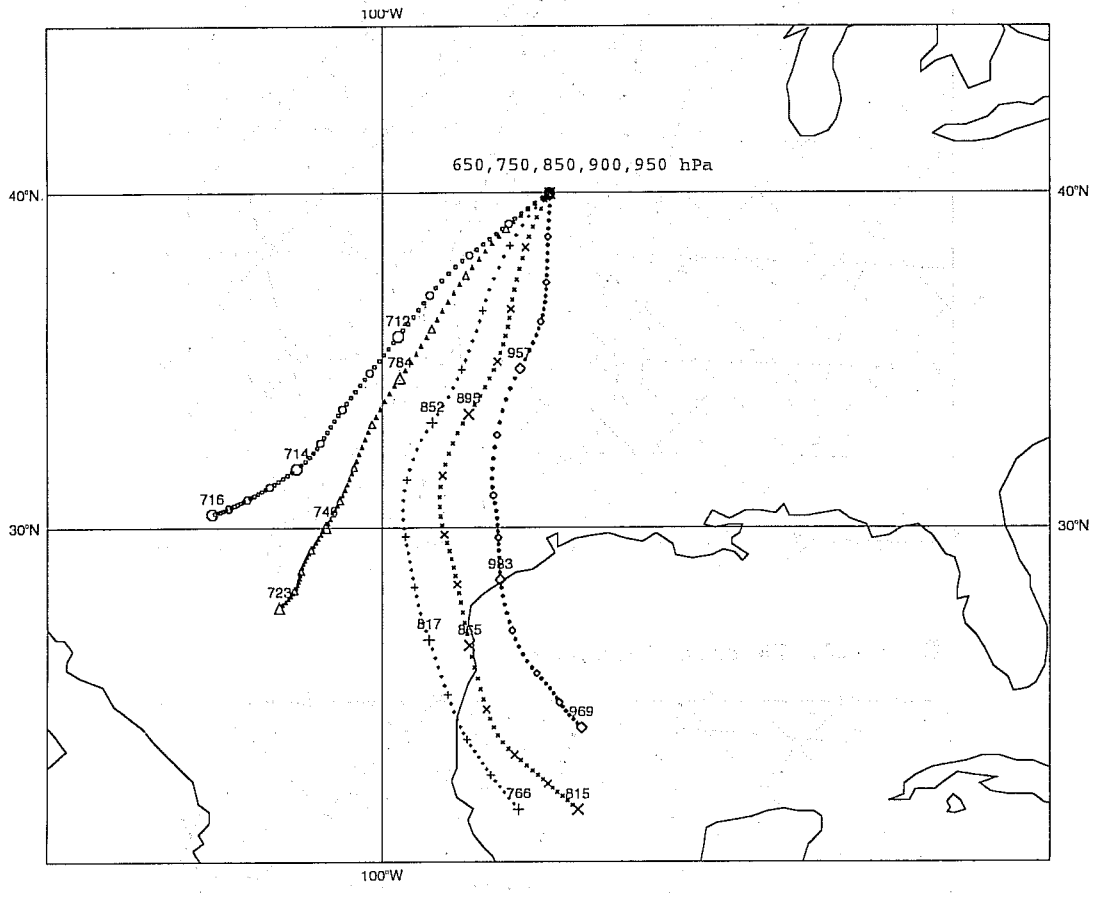


Fig 5 Three day backward trajectories from location 40 N, 95 W at the levels 950, 900, 850, 750 and 650 hPa. The fields at successive forecast ranges 72, 66, 60, ... 12, 6, 0 hours, averaged between verifying dates 9 to 25 July, have been used for the computation of these trajectories. The printed numbers along the trajectories indicate the pressure height at one day intervals.

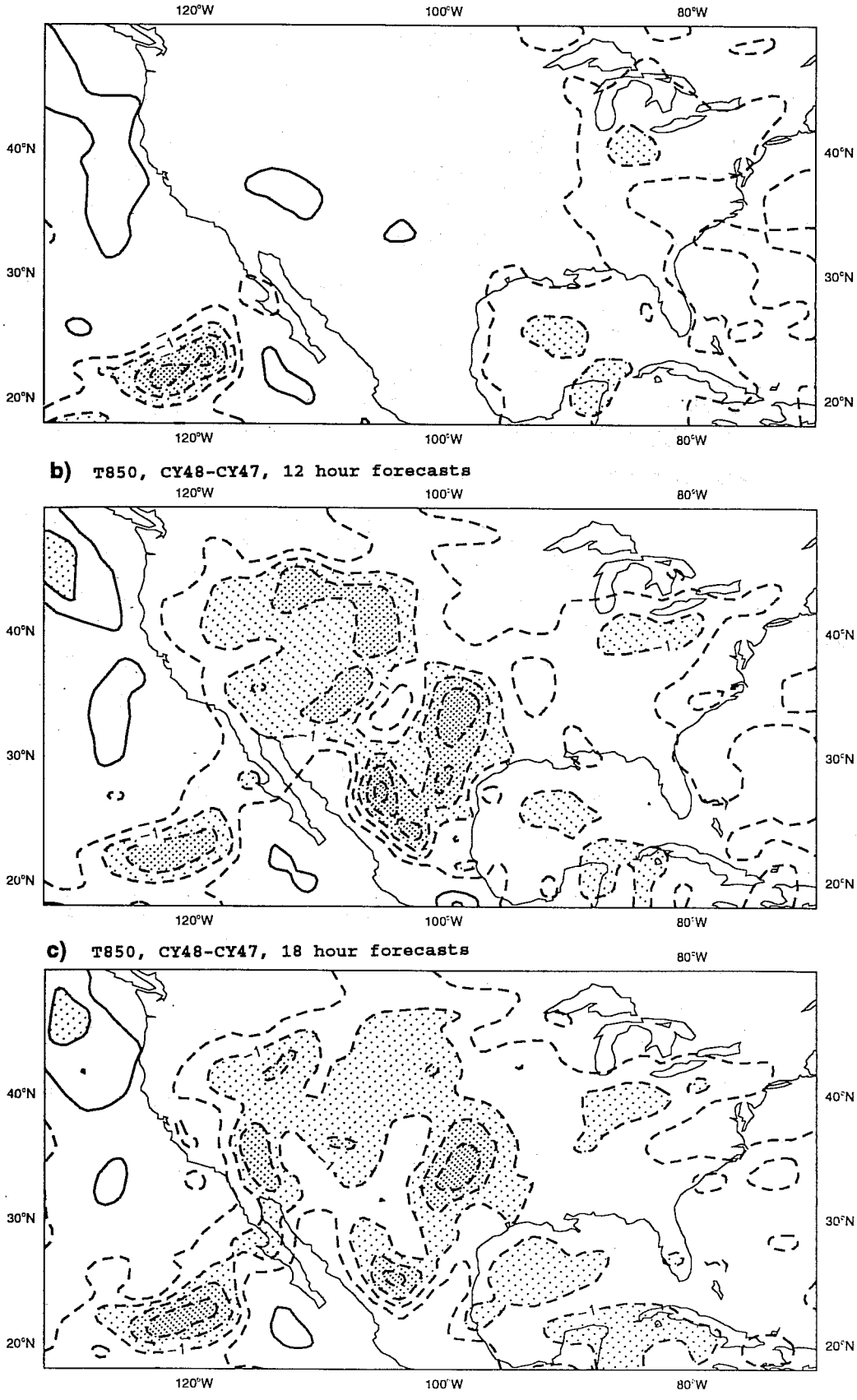


Fig 6 Evolution of the temperature difference between CY48 and CY47 at model level 26 (about 850 hPa) during the forecast up to 30 hours. The differences have been averaged over all forecasts verifying between 9 and 25 July. Negative values have dashed contours; the contour interval is 0.5 K with shading above 1 K difference.

**d)** T850, CY48-CY47, 24 hour forecasts

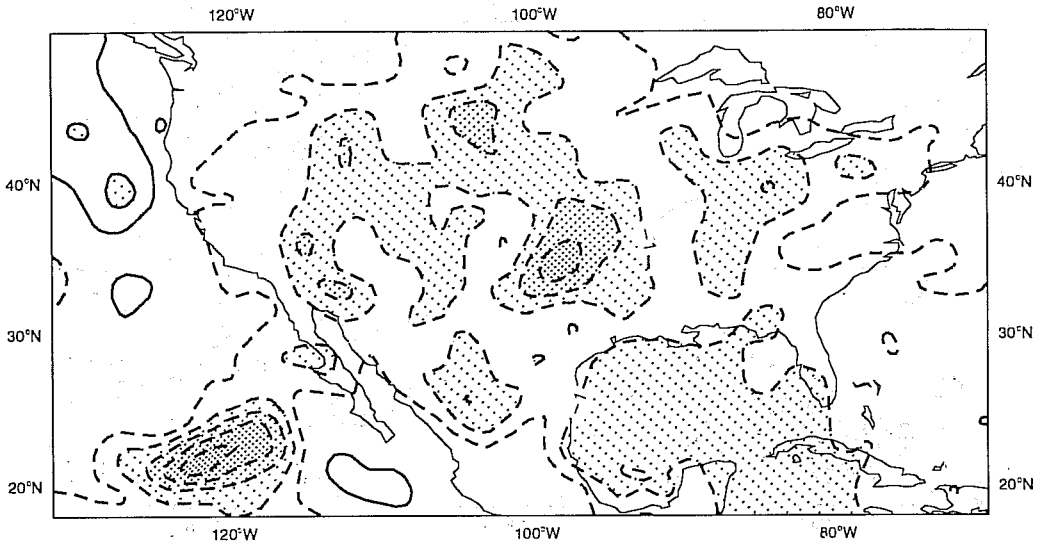


**e)** T850, CY48-CY47, 30 hour forecasts

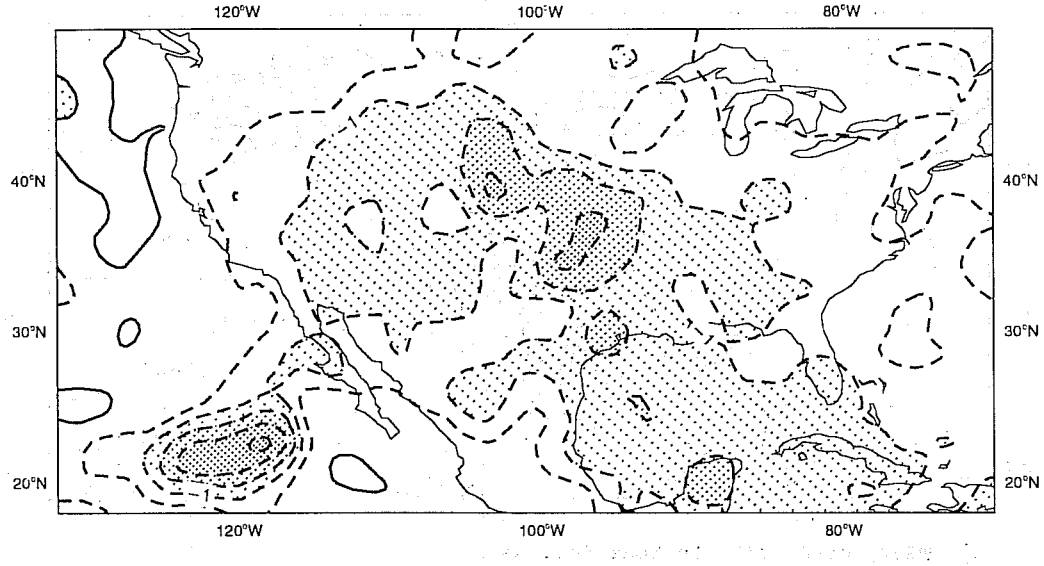


Fig 6 cont.

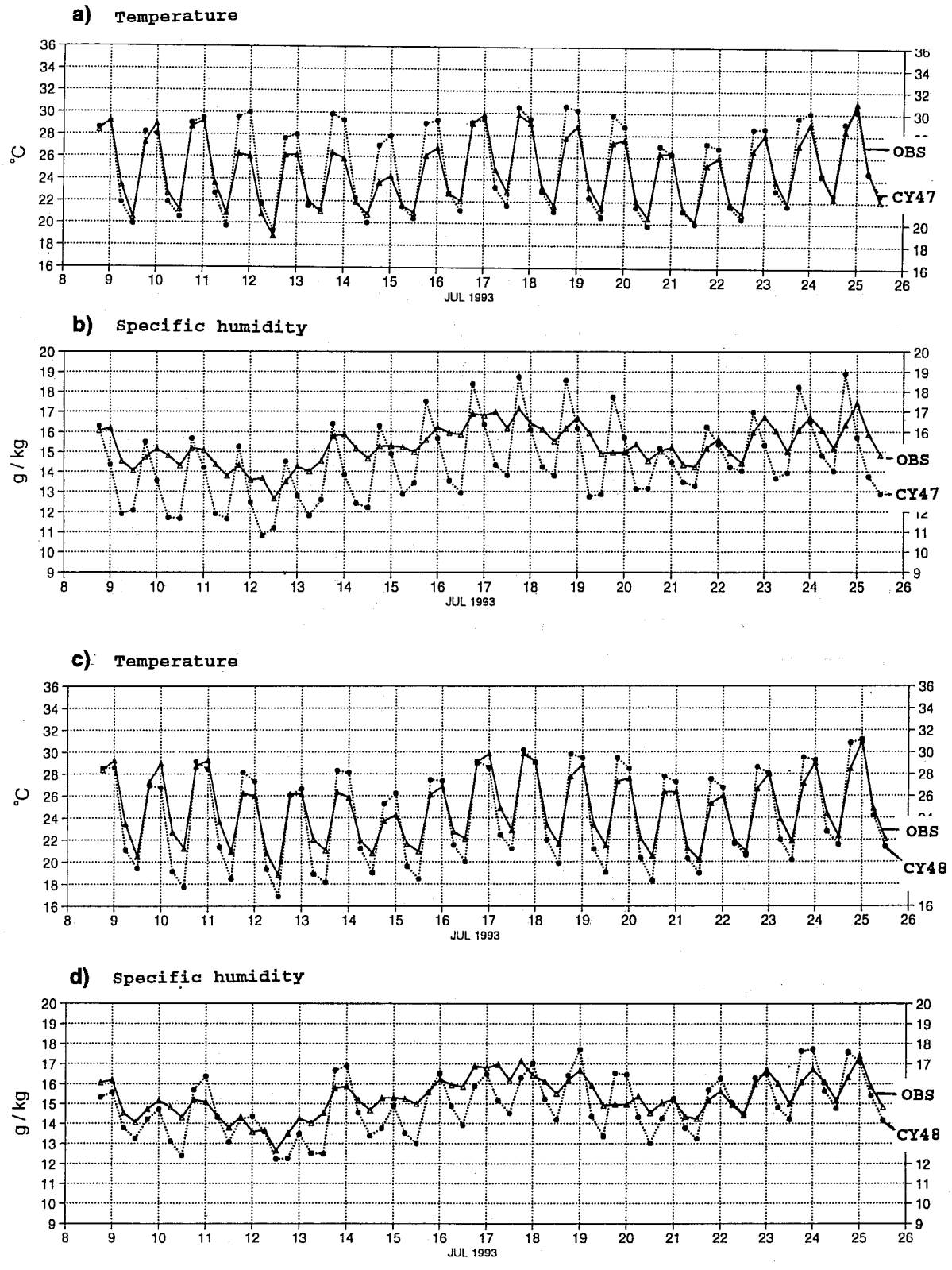


Fig 7 Time series of temperature (A,C) and specific humidity (B,D) averaged over all SYNOP stations in the area 35-45 N and 90-100 W. The dotted lines are 54, 60, 66 and 72 hour forecasts from successive analysis at 12 UTC with CY47 (A,B) and CY48 (C,D). The solid lines are observations.

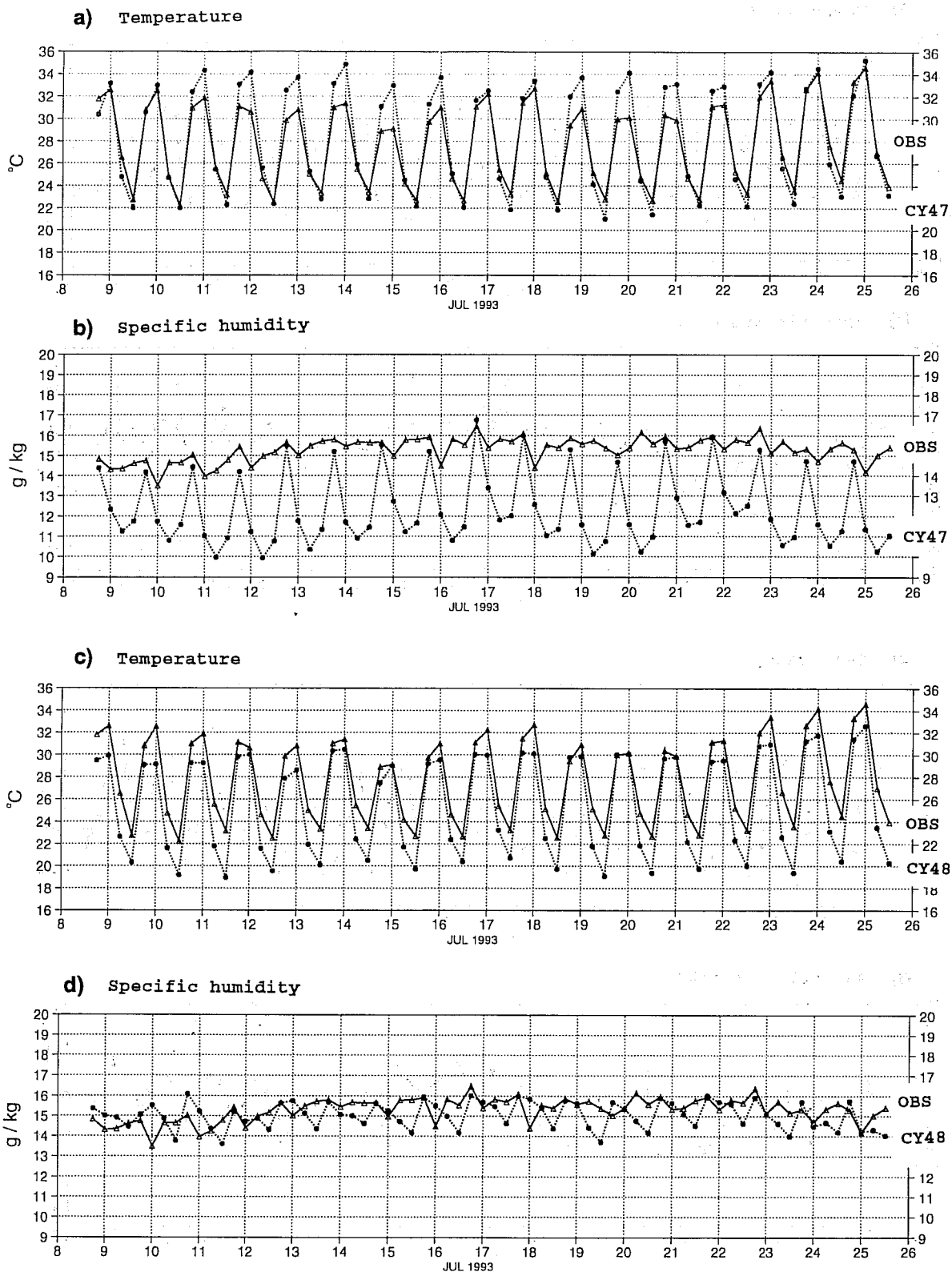


Fig 8 As Fig 7 for the area between 28-38 N and 93-103 W.

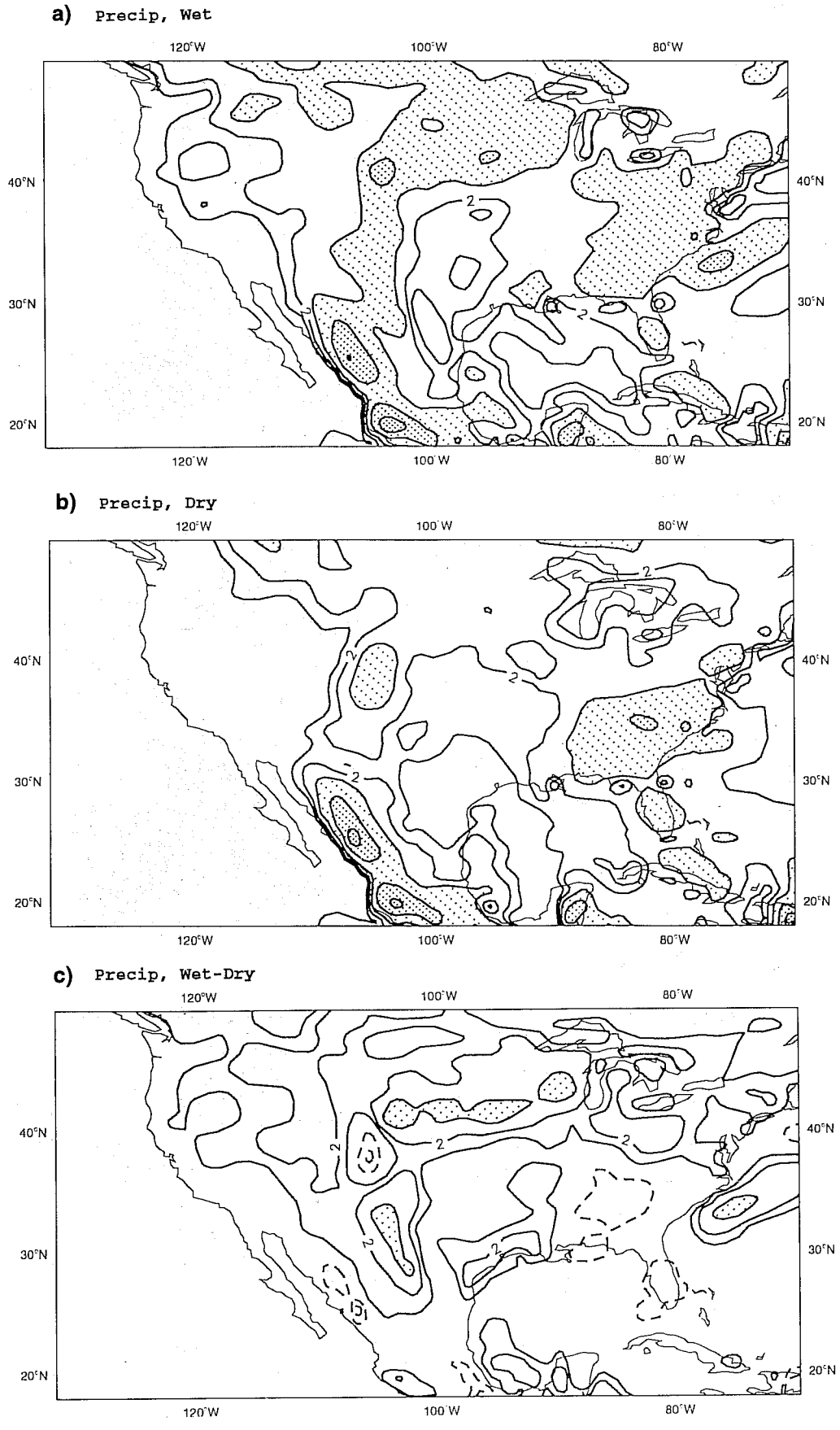


Fig 9 Precipitation averaged over an ensemble of 3 thirty day forecasts at T106L31 resolution with CY48. Fig (A) is with wet initial soil moisture, Fig (B) with dry initial condition and (C) is the difference between wet and dry. Contours are at 1, 2, 4, 8, ... mm/day with shading above 4 mm/day.

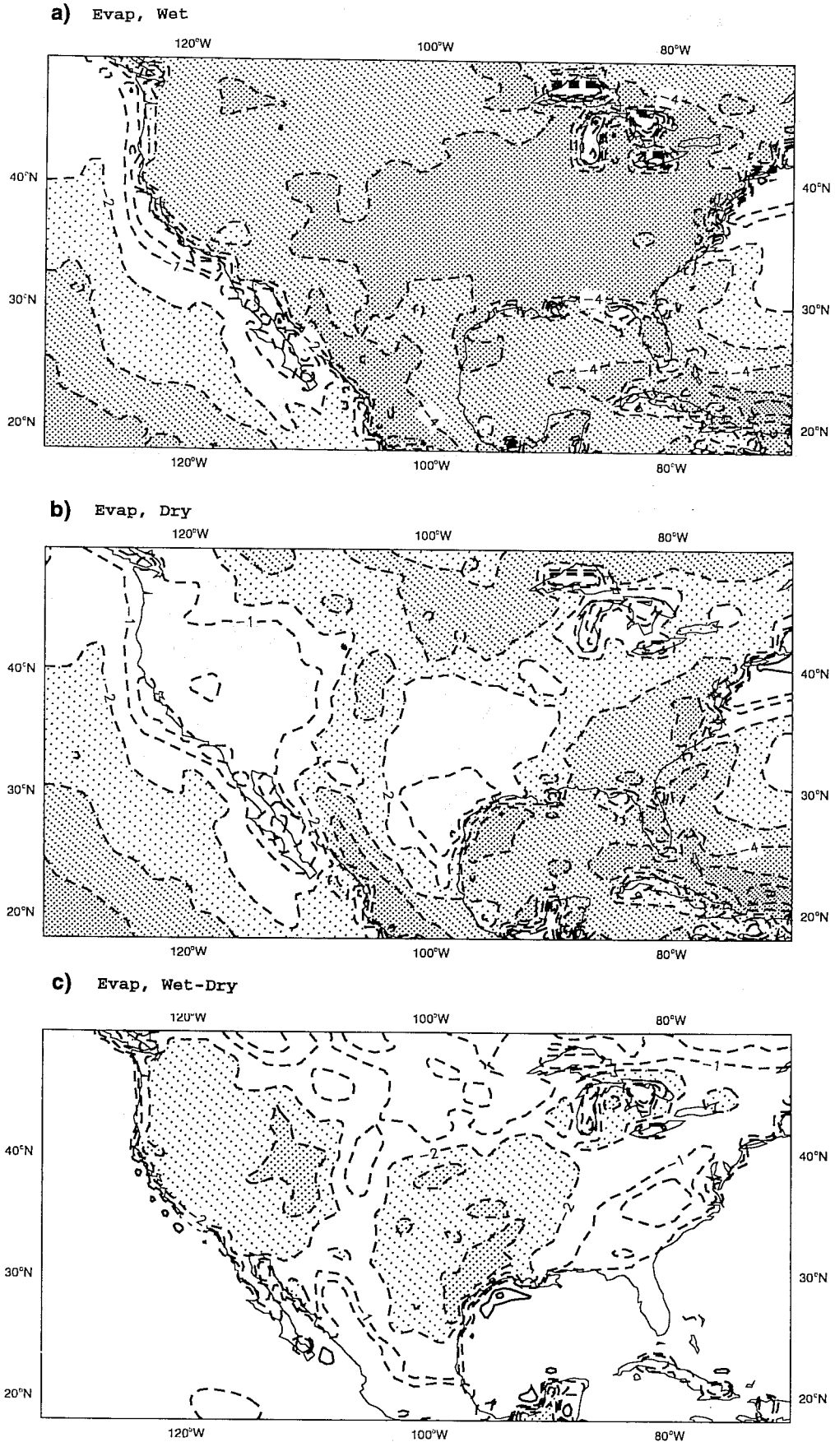


Fig 10 As Fig 9 for evaporation. Contours are at 0.5, 1, 2, 3, ... mm/day with shading above 2 mm/day.

a) Wet

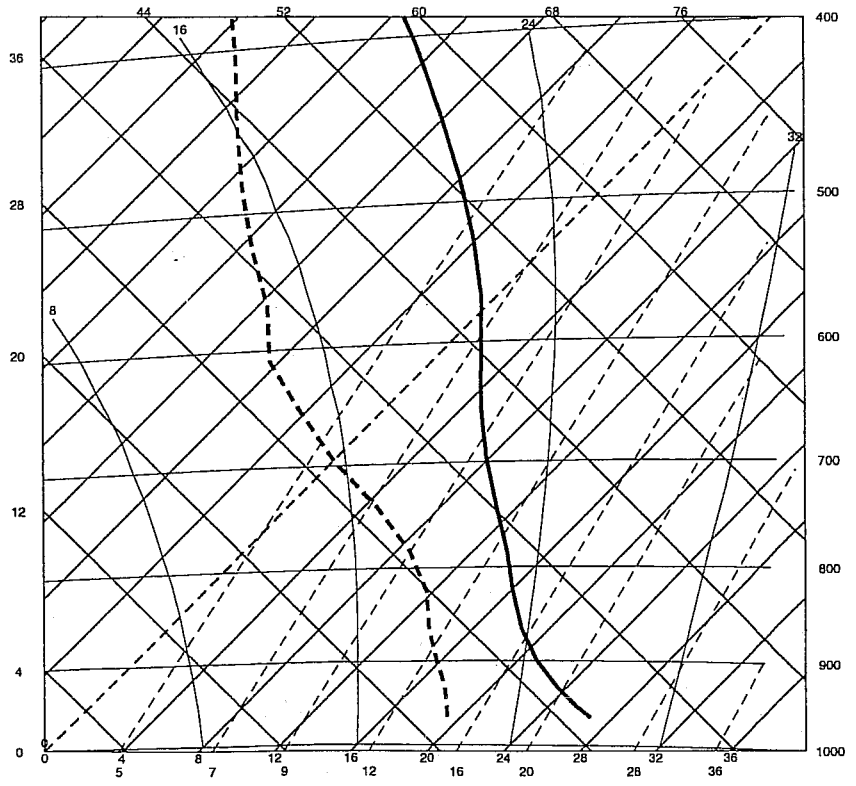


b) Dry

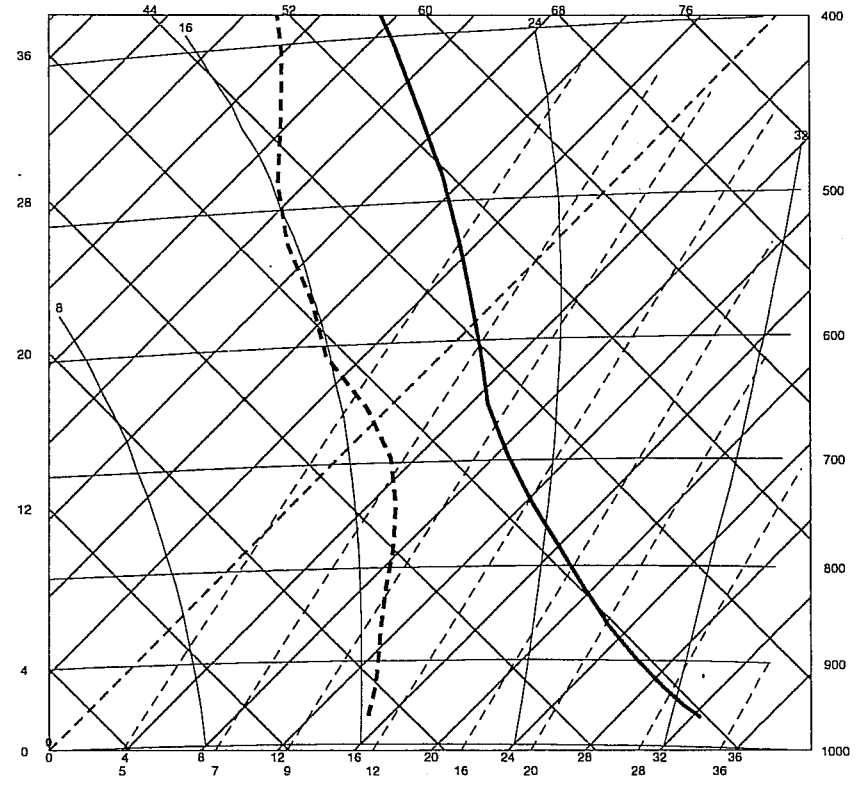


Fig 11 Thermodynamic profiles at 40 N, 95 W for 18 UTC averaged over 30 days. Fig A represents the average of 3 members of an ensemble of 30 day integrations from a wet soil initial condition, Fig B similarly from a dry soil initial condition, and Fig C shows the operational analysis of July 1993.

c) Operational analysis

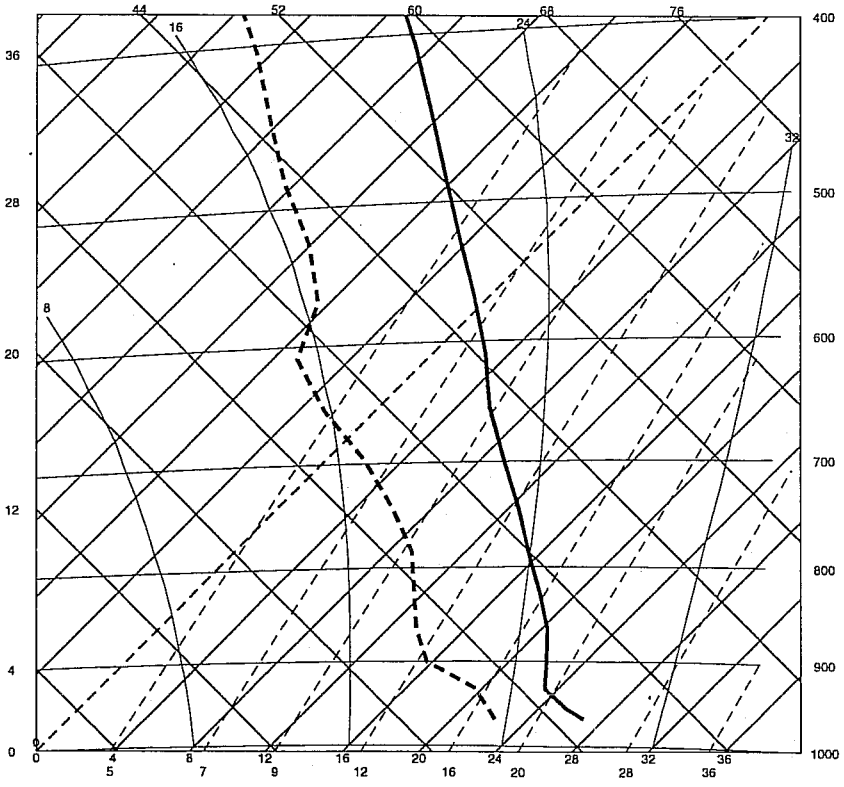


Fig 11 cont.

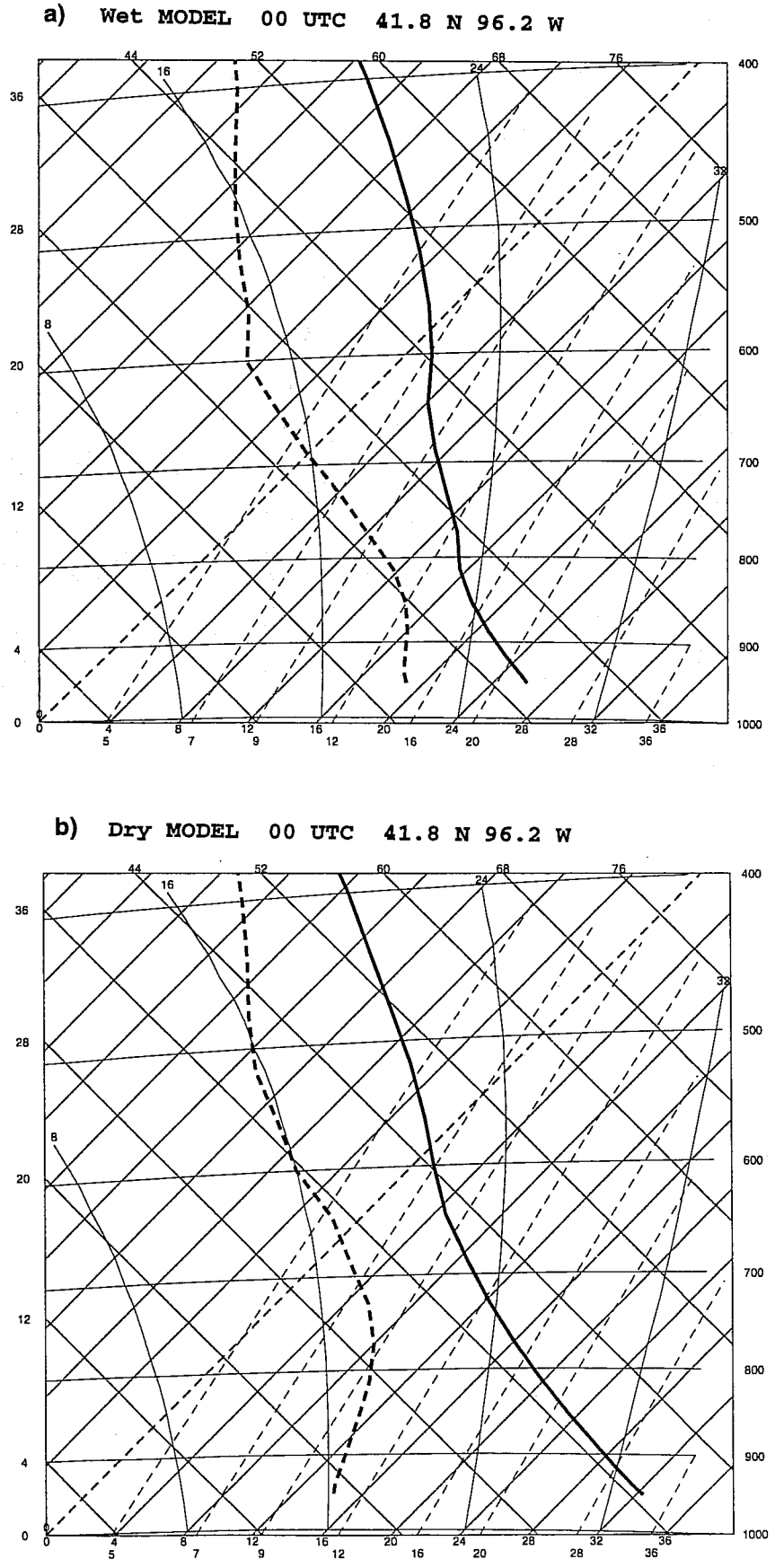


Fig 12 Thermodynamic profiles near radio sonde station 72553 for 0 UTC averaged over 30 days. Fig A represents the average (at the nearest grid point) of 3 members of an ensemble of 30 day integrations from a wet soil initial condition, Fig B similarly from a dry soil initial condition and Fig C shows the July average of the radiosonde.

c) RADIO SONDE 00 UTC 41.4 N 96.0 W

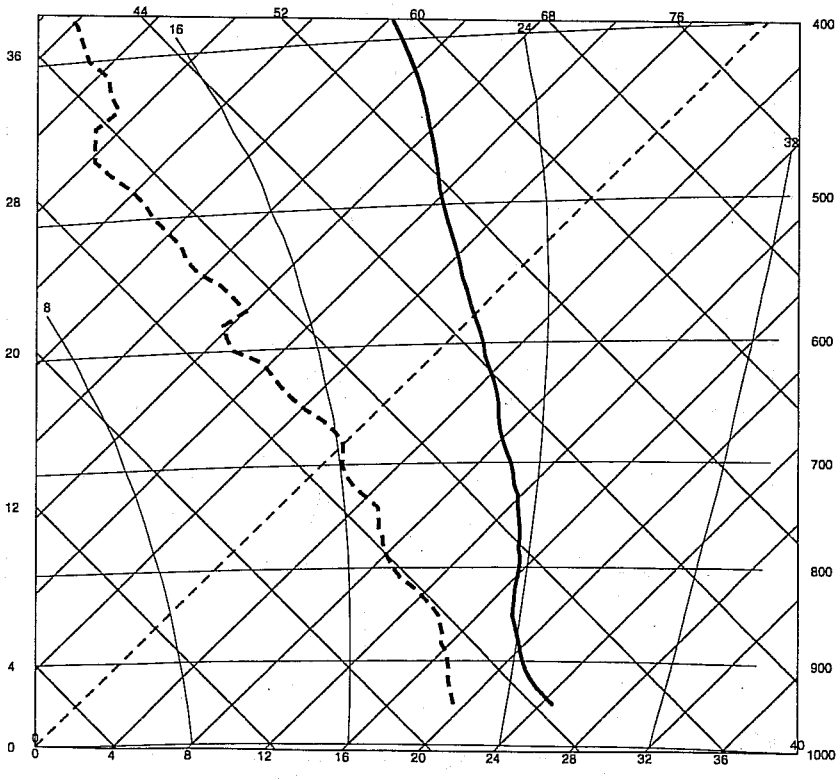


Fig 12 cont.

a) Wet MODEL 00 UTC 39.6 N 95.6 W

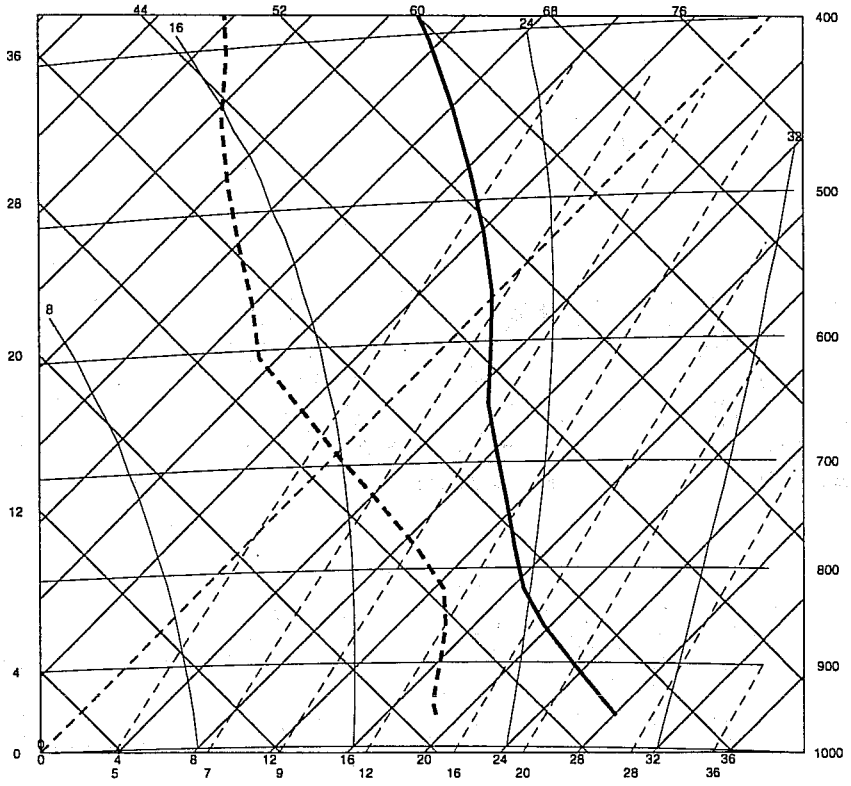


b) Dry MODEL 00 UTC 39.6 N 95.6 W

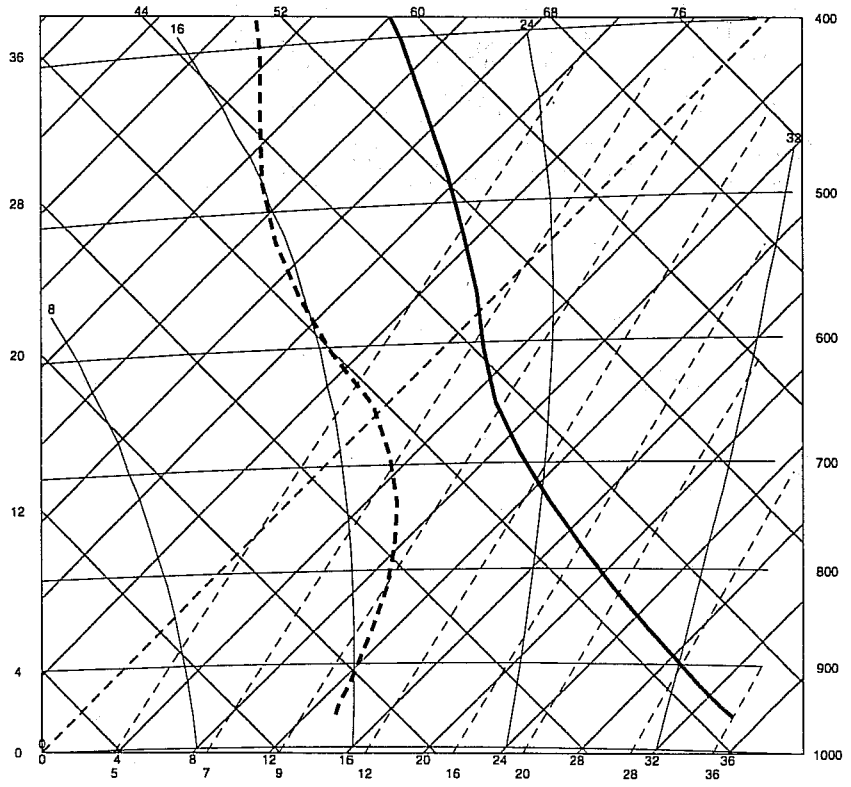


Fig 13 As Fig 12 for radiosonde station 72456.

c) RADIO SONDE 00 UTC 39.1 N 95.6 W

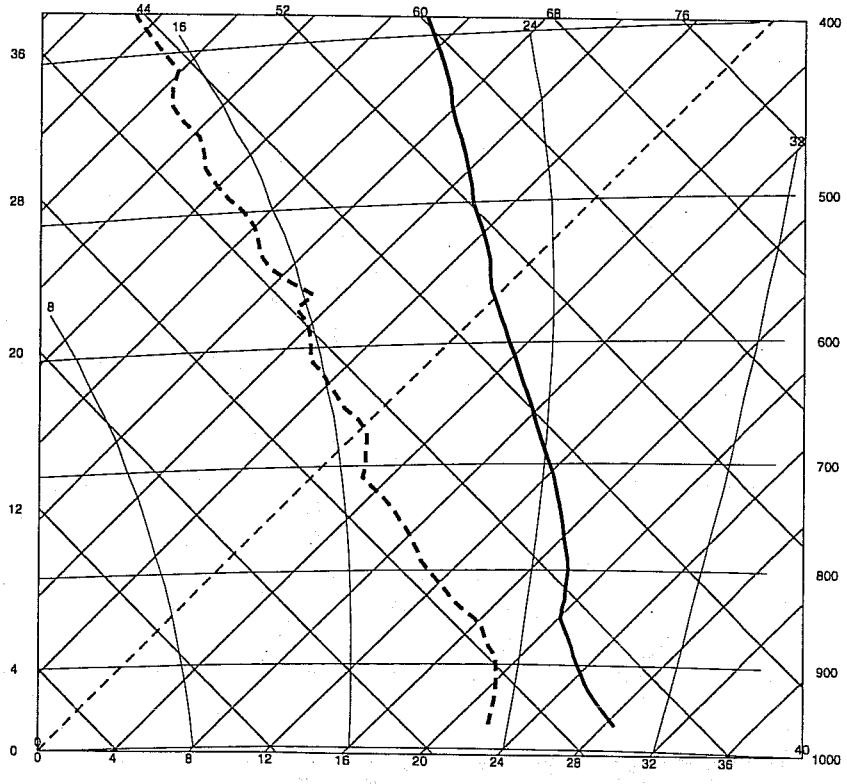


Fig 13 cont.

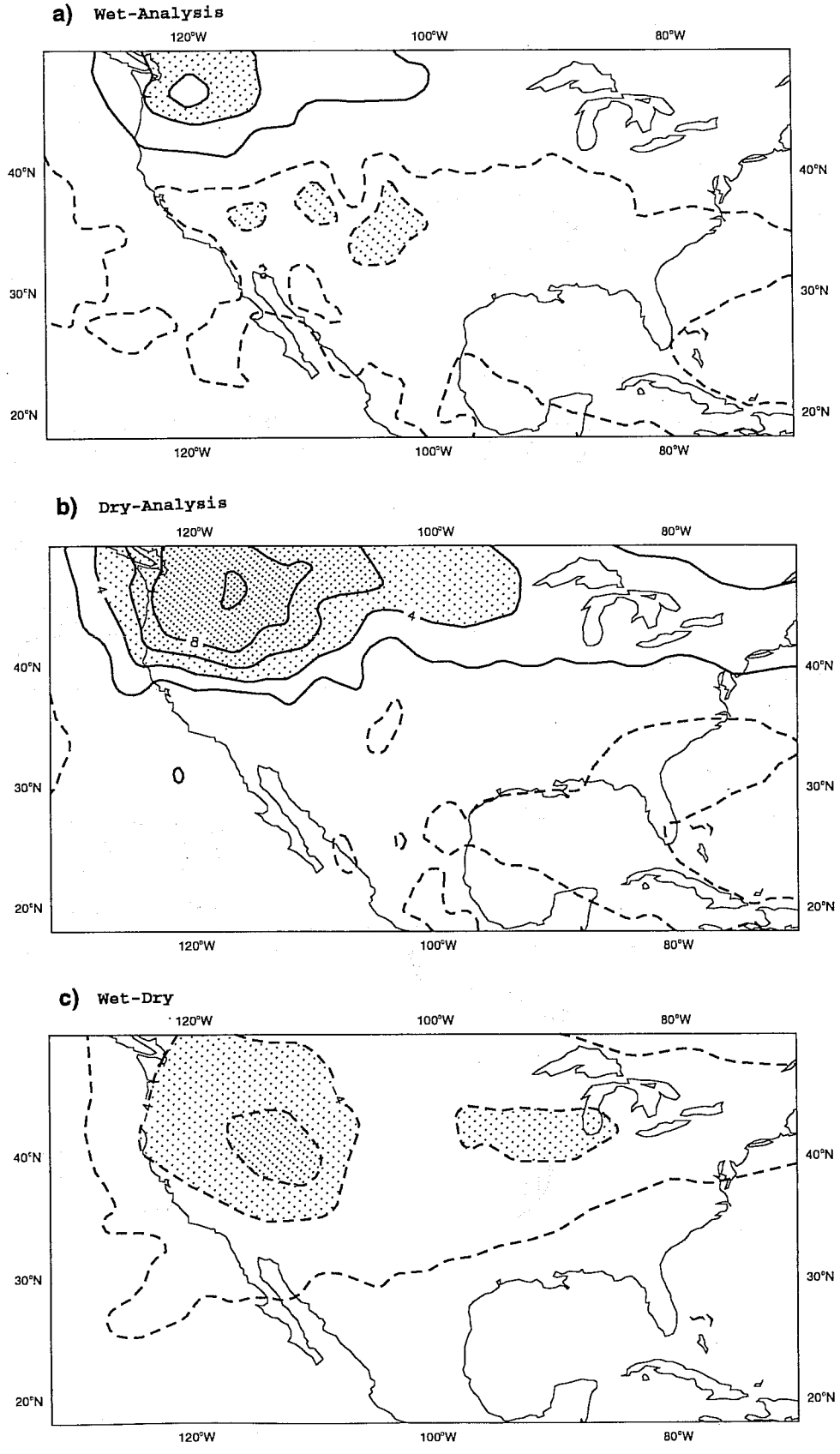


Fig 14 Temperature difference at level 26 (about 850 hPa) between the ensemble of wet 30 day integrations and the operational analysis (A), between the dry integrations and the analysis (B) and the difference between the wet and the dry integrations (C). The forecasts have been averaged over the three members of the ensemble and 30 days; the analysis has been averaged over July 1993. The contour interval is 2 K.

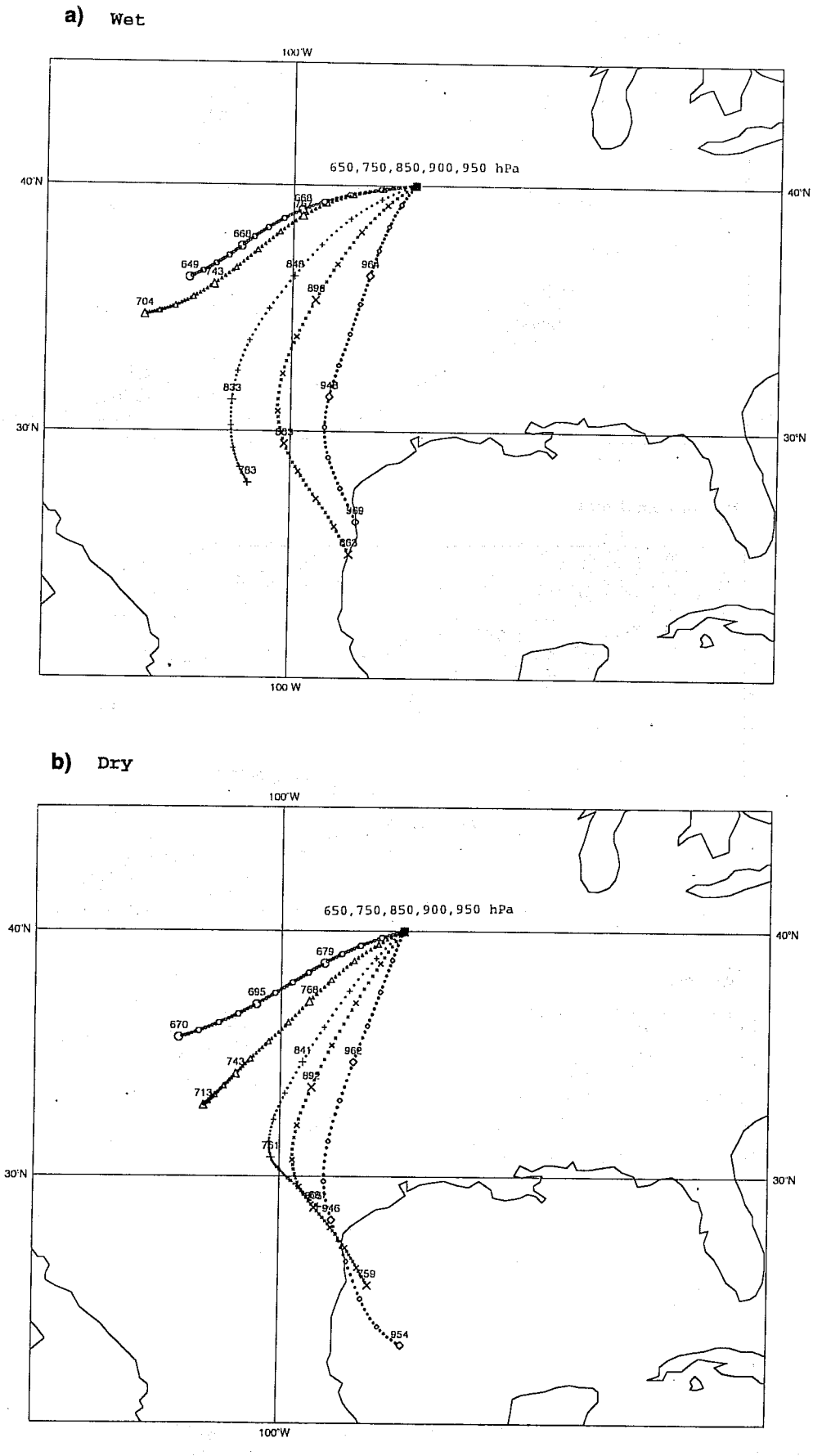


Fig 15 Backward trajectory over three days computed from the flow field of wet (A) and dry integrations (B) averaged over 30 days and the three members of the ensemble.